

**A novel curved-corrugated channel: Thermal-hydraulic performance and design parameters with nanofluid**

Submitted By

**Rifat Ahamed**

180011222

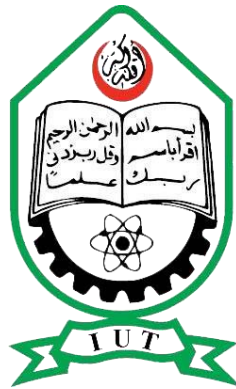
**Maisha Nusrat**

180011207

Supervised By

**Dr. Mohammad Monjurul Ehsan**  
Associate Professor

**A Thesis submitted in partial fulfillment of the requirement for the degree of Bachelor of Science in Mechanical Engineering**



**Department of Mechanical and Production Engineering (MPE)**

**Islamic University of Technology (IUT)**

**May, 2023**

### Candidate's Declaration

This is to certify that the work presented in this thesis, titled, “**A novel curved-corrugated channel: Thermal-hydraulic performance and design parameters with nanofluid**”, is the outcome of the investigation and research carried out by me under the supervision of **Dr. Mohammad Monjurul Ehsan, Associate Professor, Islamic University of Technology**.

It is also declared that neither this thesis nor any part of it has been submitted elsewhere for the award of any degree or diploma.

-----

Rifat Ahamed

Student No: 180011222

Maisha Nusrat

Student No: 180011207

## RECOMMENDATION OF THE BOARD OF SUPERVISORS

---

The thesis titled “**A novel curved-corrugated channel: Thermal-hydraulic performance and design parameters with nanofluid**” submitted by **Rifat Ahamed**, Student No:**180011222** and **Maisha Nusrat**, Student No:**180011207** has been accepted as satisfactory in partial fulfillment of the requirements for the degree of B Sc. in Mechanical Engineering on **17<sup>th</sup> January, 2023**.

## BOARD OF EXAMINERS

---

1. -----

Dr. Mohammad Monjurul Ehsan  
Associate Professor  
MPE Dept., IUT, Board Bazar, Gazipur-1704, Bangladesh.

(Supervisor)

## ABSTRACT

In the present study, the impact of nanofluids has been analyzed in a corrugated channel with baffles. The primary objective of this study is to evaluate the thermodynamic performance of both single and hybrid nanofluids in relation to different Reynolds numbers and nanoparticle volume concentrations for the corrugated pipe. The unique design of the corrugation has a chance to enhance the heat transfer rate. For a uniform heat flux on the surface wall, numerical simulations are conducted for different element sizes while the Reynolds no is held constant. Performance analysis of hybrid nanofluids  $Al_2O_3-CuO$  and  $TiO_2-SiO_2$  has been carried out. The thermophysical properties of nanofluids have been calculated using various correlations. Computational fluid dynamics (CFD) simulations are performed to gain insights into the flow and thermal behavior inside the corrugated pipe. These simulations provide detailed information on velocity profiles, temperature gradients, and pressure distributions, facilitating a comprehensive understanding of the heat transfer mechanisms involved. The findings of this research demonstrate that the implementation of corrugated pipe significantly enhances heat transfer performance compared to traditional smooth pipes. The increased surface area provided by the corrugations promotes enhanced convective heat transfer, while also altering flow characteristics to maximize thermal efficiency. A parametric study on the E shaped baffles has been carried out to show the change in the Thermo-hydraulic performance and fluid nature in the pipe.

# TABLE OF CONTENT

<b>ABSTRACT</b> .....	1
<b>NOMENCLATURE</b> .....	5
<b>Chapter 1: Introduction</b> .....	6
<b>OBJECTIVES</b> .....	6
<b>STRUCTURE OF THE THESIS</b> .....	6
<b>CORRUGATED PIPE WITH E SHAPED BAFFLES</b> .....	7
<i>Effect of Baffles and Corrugation</i> .....	7
<i>Heat Transfer Enhancement Techniques</i> .....	8
<i>Nanofluid for heat transfer enhancement</i> .....	9
<i>Effect of hybrid nanofluid</i> .....	10
<i>Physical model</i> .....	11
<b>BOUNDARY CONDITIONS AND ASSUMPTIONS</b> .....	12
<b>Chapter 2: Computational Methodology</b> .....	15
<b>GOVERNING EQUATIONS</b> .....	15
<b>PERFORMANCE PARAMETERS AND DIMENSIONLESS NUMBERS</b> .....	18
<b>NUMERICAL IMPLEMENTATION</b> .....	20
<b>MESH GENERATION AND GRID INDEPENDENCE ANALYSIS</b> .....	20
<b>CODE VALIDATION</b> .....	24
<b>THERMOPHYSICAL PROPERTIES OF NANOFUIDS</b> .....	26
<b>Chapter 3: Result and Discussion</b> .....	29
<b>RESULT AND DISCUSSION</b> .....	29
<b>Effect of Nanofluid</b> .....	29
Effect of blockage ratio.....	31
<b>FLOW BEHAVIOR INVESTIGATIONS</b> .....	36
<b>Chapter 4: Conclusion</b> .....	42
<b>Chapter 5: References</b> .....	43

## LIST OF FIGURES

- Figure 2: Schematic diagram of the computational domain.....19
- Figure 3: Mesh generation at tube's cross section and along its length.....26
- Figure 4: Section view of the tube along its length.....27
- Figure 5: Different views of mesh with inflation layer.....32
- Figure 6: Pressure contour along the length of the tube for nanofluid.....37
- Figure 7: Temperature profile of tube along the length for nanofluid.....37
- Figure 8: Surface Nusselt no profile along the tube for nanofluid.....38
- Figure 9: Velocity streamline with nanofluid ZnO-water.....39
- Figure 10: Velocity streamline with water.....40

## LIST OF TABLES

- **Table 1.....16**
- **Table 2.....28**
- **Table 3.....35**
- **Table 4.....35**

## NOMENCLATURE

$\vec{a}$ .....nanoparticles acceleration,  $\text{ms}^{-2}$

**A**.....area,  $\text{mm}^2$

**BR**.....blockage ratio,  $\frac{e}{w_b}$

**c1, c2, C $\mu$ ,  $\sigma_k$ ,  $\sigma_\varepsilon$** .....model constants

**C $p$** .....specific heat capacity (J/kg. K)

**D**.....diameter of corrugation, mm

**D $_h$** .....hydraulic diameter, mm

**e**.....width of baffle, mm

*f $_{drag}$* .....drag function

**g**.....acceleration of gravity,  $\text{m.s}^{-2}$

**G**.....generation of turbulent kinetic energy,  $\text{kg/ms}^3$

**h $_b$** .....height of baffle, mm

**H**.....height of channel, mm

**HTC**.....heat transfer coefficient, ( $\text{W/m}^2. \text{K}$ )

**V $_{dr}$** .....drift velocity, m/s

**V $_{pf}$** .....relative velocity, m/s

**u, v, w**.....velocity component, m/s

**H**.....height of channel, mm

**I**.....turbulent intensity

**k**.....turbulent kinetic energy, ( $\text{m}^2/\text{s}^2$ )

**k**.....conduction heat transfer coefficient,  $\text{W/m.K}$

**Nu**.....Nusselt number

**P**.....pitch of corrugation, mm

**p**.....pressure, Pa

$\Delta p$ .....pressure drop, Pa

**Pr**.....Prandtl number

**PEC**.....Thermal-hydraulic performance factor

**Re**.....Reynolds number

**W**.....width of tested channel, mm

**T**.....temperature, K

**V**.....time-mean and fluctuating velocity, m/s

**X, y, z**.....cartesian x, y, z-coordinate

### Greek symbols

$\mu$  dynamic viscosity of the fluid,  $\text{kg/m. s}$

$\rho$  density,  $\text{kg/m}^3$

$\varepsilon$  Turbulent kinetic dissipation,  $\text{m}^2/\text{s}^2$

$\sigma_k$  diffusion Prandtl number for k

$\phi$  volume fraction of nanoparticle

### Subscripts

**av** average

**b** baffle

**corr** corrugated

**in** inlet

**m** mean

**mod** modified

**f** fluid

**nf** nanofluid

**np** nanoparticles

**ref** smooth channel

**out** outlet

**w** wall



# Chapter 1: Introduction

## OBJECTIVES

The objectives of your thesis project may include:

1. Investigating the thermophysical properties (such as thermal conductivity, viscosity, and heat capacity) of the nanofluid in the pipe.
2. Determining how these properties change as a function of temperature and/or concentration of nanoparticles in the fluid.
3. Examining the effect of the nanoparticles on the heat transfer performance of the tube.
4. Analyzing the stability and potential agglomeration of the nanoparticles in the fluid.
5. Developing a mathematical model to predict the thermophysical properties and heat transfer performance of the tube with nanofluid.
6. Comparing the results with the base fluid and other nanoparticle

## STRUCTURE OF THE THESIS

In this project 2 different types of geometry have been analyzed in order to find the thermophysical properties with the usage of different types of nanofluid.

The project works on a corrugated pipe with baffles. It has its own literature review with appropriate references and boundary condition. This section should provide background information on the topic, including the importance of studying thermophysical properties and heat transfer in nanofluids, the current state of research in the field, and the specific research question or hypothesis being addressed in the thesis.

## **CORRUGATED PIPE WITH E SHAPED BAFFLES**

The use of mechanical applications in the industrial field often requires high thermal performance. To meet this requirement, researchers have been working to improve thermal efficiency through the use of modern technology and different designs. This has led to the optimization of materials and designs for thermal devices, making them smaller and more cost-effective. Curved channels are widely used in various industries, including aerospace, astronautics, nuclear reactor design, and electrical and electronic packaging cooling. To improve heat transfer, researchers have employed various techniques such as roughened surfaces and turbulators. Baffles and corrugations are considered particularly effective methods for enhancing heat transfer by interrupting hydrodynamic and thermal boundary layers. This leads to flow separation and recirculation, which increases the impingement of the channel wall downstream of each baffle or corrugation, leading to improved heat transfer. Conventional fluids often have poor thermal conductivity, leading to weak thermal performance. To address this, researchers have been exploring the use of nanofluids, which are created by adding nanoparticles to base fluids, as an effective passive approach to enhance thermal properties and heat transfer.

### ***Effect of Baffles and Corrugation***

Numerical studies have shown that the use of vortex flow can significantly increase the rate of heat transfer in channels, according to research by Promvonge et al. [1]. They also proposed empirical correlations for the Nusselt number and friction factor for tubes with oblique baffles [2]. Sahel et al. [3] numerically evaluated the performance of a new baffle configuration in a channel and found that it resulted in an improvement in heat transfer ranging from 2% to 65% compared to a standard baffle. Khanlari et al. [4] experimentally and numerically tested solar air collectors with different baffle designs and found that the parallel-pass collector with double baffles achieved the highest thermal efficiencies between 71.12% and 75.11%. Similarly, Fiuk and Dutkowski [5] added waveshape baffles to a solar air collector and reported a maximum efficiency of 73.8%. On the other hand, Cabonce et al. [6] tested a small triangular corner baffle system within a box culvert barrel and found that it had a moderate effect on flow resistance and discharge capacity. Wang and Smith [7] used baffles in redox flow battery tanks and found that they were necessary to improve performance. Previous studies have shown that turbulent fluid

flow and heat transfer through a backward-facing step in combination with various corrugated walls can result in improved thermal efficiency. Hilo et al. [8] studied the turbulent fluid flow and heat transfer through a wavy channel, and Zhao et al. [9] conducted experiments, numerical simulations, and analytical analyses to study the effects of corrugated channels on thermal efficiency. Afrouzi et al. [10] identified that the Reynolds number, amplitude of pulses, and power law index are crucial factors that influence the behavior of pulsating flow through corrugated channels. Using CFD simulations, Zhu and [11] studied and modeled two-phase flows (liquid-gas) through corrugated walls and developed new correlations for pressure drop calculations. Chaudhury and Raju compared the thermal output of a corrugated wavy channel with a straight channel under laminar flow conditions and found that the corrugated channel exceeded the straight rectangular channel by about 47.8% in terms of Nusselt number. Alnak [12] used numerical simulations to investigate the heat transfer characteristics of corrugated channels with rectangle baffles under Reynolds number ranges from 1000 to 6000. Ünal et al. [13] used particle image velocimetry to study the flow between corrugated walls with periodic grooves and observed strong hydrodynamic interactions among successive corrugations. Naphon [[14–16] studied numerically and experimentally the effect of corrugated walls on heat transfer and found a significant improvement. Miroshnichenko et al. [17] performed a numerical analysis of laminar mixed convection of micropolar fluid in a horizontal wavy channel and found that the average Nusselt number decreases with increasing undulation number while the influence of vortex viscosity parameter is non-monotonic.

### ***Heat Transfer Enhancement Techniques***

Heat transfer enhancement techniques refer to methods used to increase the rate of heat transfer in a given system. These techniques are often used in industrial and engineering applications, such as in heat exchangers and heat sinks, to improve the efficiency of the system and reduce energy costs.

One common heat transfer enhancement technique is the use of fins. Fins are extended surfaces that are attached to a heat-generating component, such as a pipe or a solid block. The fins increase the surface area of the component, which allows for more efficient heat transfer to the surrounding air or fluid. Another technique is the use of turbulence promoters, such as vortex

generators, which are small protuberances or devices that are placed on a surface to create turbulent flow. The turbulent flow increases the heat transfer coefficient by increasing the rate of convection.

Another technique is the use of heat pipes, which are devices that use a liquid-vapor phase change to transport heat from one location to another. Heat pipes are highly effective at transferring heat due to their high thermal conductivity and large surface area. Additionally, a technique called forced convection can be used to enhance heat transfer, this is done by using fans or pumps to force a fluid over a heat-generating surface. This increases the heat transfer coefficient by increasing the fluid velocity and turbulence.

Another technique is using phase-change materials (PCM) as thermal energy storage medium, PCM's absorb or release large amounts of heat during phase change, thus increasing the heat transfer rate.

Lastly, using nano-fluids, which are suspensions of nano-sized particles in a fluid, can enhance heat transfer. The small size of the particles increases the effective thermal conductivity of the fluid, leading to an increase in the heat transfer coefficient. It's important to note that the heat transfer enhancement technique that is best suited for a particular application depends on the specific conditions of the system, including the fluid properties, the temperature range, and the desired heat transfer rate.

### ***Nanofluid for heat transfer enhancement***

One of the major obstacles to improving the efficiency of heat exchangers is the poor thermal conductivity of conventional coolants. Conventional heat transfer fluids such as water, ethylene glycol, pumping oil, and others have not demonstrated significant capabilities for cooling. To overcome these limitations, incorporating nanoparticles into a traditional fluid can be considered as a way to enhance the heat transfer capacity of these fluids. Many studies have shown that the thermal performance of nanofluids is superior to that of conventional fluids [[18–21]]. The introduction of a new type of heat transfer fluid is a result of innovation in material engineering which has enabled the production of nano-sized particles. Choi and Eastman coined the term

"nanofluid" to define this type of fluid for heat transfer that incorporates nanoscale metallic or non-metallic particles. Nanofluids have been used to improve the thermophysical properties of traditional heat transfer fluids. The dispersion of nanoparticles can significantly improve the thermal conductivity of the base fluid, thus enhancing the convective heat transfer rate [[22]]. Rostamani et al. [[23]] conducted an analysis of the heat transfer properties of nanofluids in a smooth channel. They studied three different forms of nanofluids, CuO-water, Al<sub>2</sub>O<sub>3</sub>-water and TiO<sub>2</sub>-water and considered a nanoparticle volume fraction of 0-6% and a Reynolds range of 20,000-100,000. They found that compared to Al<sub>2</sub>O<sub>3</sub> and TiO<sub>2</sub>-water nanofluids, the average Nusselt number for CuO-water nanofluids was higher, but the shear stress was also increased. Moshizi et al. [24] studied the properties of Al<sub>2</sub>O<sub>3</sub>-water nanofluid using constant heat flow in a pipeline and observed that slip velocity on the pipe wall initiates the heat transfer and pressure gradients work more effectively.

### ***Effect of hybrid nanofluid***

The incorporation of nanoparticles into traditional heat transfer fluids, known as nanofluids, has been shown to improve their thermal performance. However, recent studies suggest that combining multiple types of solid particles with traditional fluids, known as hybrid nanofluids, can result in even greater enhancement of heat transfer properties. Researchers have found that the use of hybrid nanofluids leads to improved thermal characteristics compared to using single nanoparticle nanofluids [25,26]. For example, Sumit et al. conducted an investigation of the effect of taper wire coil turbulators with various configurations on the use of hybrid nanofluids and found that it resulted in an increase in Nusselt number by approximately 47%, 71%, and 84%, and friction factor by approximately 46%, 58%, and 68% respectively. [27] Other studies also have demonstrated significant enhancement in heat transfer capabilities of hybrid nanofluids due to the combination of multiple particles that permit the construction of suitable thermal interfaces inside the fluid flow [28]. Suresh et al. [29] found that the implementation of a modest inclusion of Cu into the alumina greatly enhance heat transfer.

## ***Physical model***

Curved channels play a crucial role in a wide variety of industrial applications, from power production to chemical and food industries, electronics, environmental engineering, waste heat recovery, manufacturing, air conditioning, refrigeration, and space technology. In this numerical study, a new curved channel design is introduced to investigate the flow and heat transfer characteristics of ZnO-water nanofluid using a two-phase mixture method. The proposed model includes a corrugated upper wall and a smooth lower wall, with an average distance of 100mm between the two walls. The width and horizontal length of the channel are 200 mm and 1200 mm respectively. The corrugations on the upper wall are at a varying pitch angle. The upper wall of the channel is heated by a constant temperature, while the lower wall is kept adiabatic. The upper wall of the channel is cooled by E-shaped baffles placed inside the channel on the bottom wall, with different design parameters. The characterization of the baffle elements repeatedly inserted into the curved-corrugated channel is illustrated in Figure 2.

**Table 1**

Geometrical structure of curved-corrugated channel with baffles.

Curved-corrugated channel		
Parameter	Symbol	Value (mm, Deg)
Horizontal length of channel	L	1200
Horizontal length of Entry Region	$L_{in}$	500
Horizontal length of Fully Developed Region	$L_{out}$	1500
Vertical height of channel	H	100
Width of channel	W	200
Baffle design parameters		
Thickness	t	2
Gap ratio	GR	0.2
Pitch angle	$\beta$	10°
Vertical baffle height	$h_b$	70

Horizontal baffle width	$w_b$	80
Blockage ratio	BR	0.10,0.15,0.25

## BOUNDARY CONDITIONS AND ASSUMPTIONS

The flow velocity at the inlet boundary is set with a temperature of 300 K and a turbulence intensity of 4.61%. The pipe's wall is subject to a no-slip condition. Additionally, the walls with corrugations are exposed to a constant heat flux of 5000 kW/m<sup>2</sup> while the remaining smooth walls are not subjected to any heat. An implicit solver was chosen to solve the governing equations, and the SIMPLE algorithm was used to resolve the pressure and velocity relationship. The continuity equation, momentum equation, and energy equations were discretized using a second-order upwind scheme. To evaluate the hydrodynamic behavior, the test section was placed at a distance of 500 mm from the inlet to create a fully developed flow zone. Measurements of pressure and temperature were taken at the starting and ending points of the corrugated region, and these readings were recorded while varying the boundary inlet velocity.

At the inlet:

$$u = v = 0, w = w_{in}, T_{in} = 300K, k_{in} = \frac{3}{2(Iu_{in})^2}, \varepsilon_{in} = C_\mu^{3/4} \frac{K^{3/2}}{Lt}$$

At the Corrugated wall:

$$u = v = w = 0, \frac{\partial T}{\partial y} = 0, k = \varepsilon = 0$$

At the Outlet:

$$\frac{\partial u}{\partial z} = \frac{\partial v}{\partial z} = \frac{\partial w}{\partial z} = 0, \frac{\partial T}{\partial z} = 0, \frac{\partial k}{\partial x} = \frac{\partial \varepsilon}{\partial x} = 0$$

Some assumptions have been taken out in order to carry out the study. These assumptions are employed in the numerical simulation calculations:

- The flow is in a three-dimensional steady state and fully developed flow.
- The gravitational force is negligible.
- The velocity profile of the inlet pipe is considered to be uniform.
- No slip condition in the wall
- The heat loss to the environment is negligible.
- Nano-fluid was considered Newtonian and incompressible.
- The thermophysical properties of hybrid nanofluids are stable and temperature independent.
- Natural convection is insignificant.



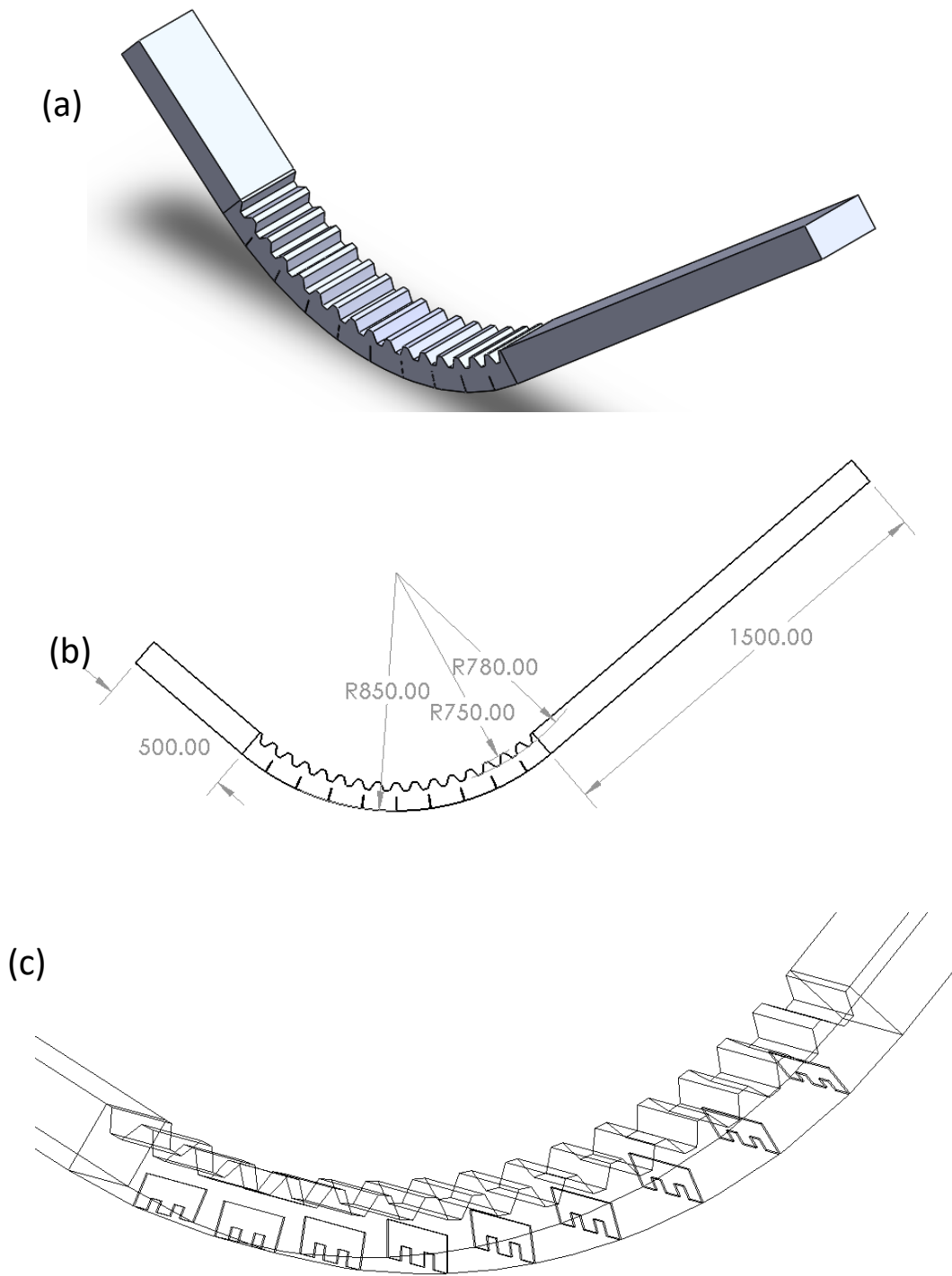


Figure 1: Schematic diagram of the computational domain: (a) Geometrical model of curved-corrugated channel, (b) Baffle geometry, and (c) Channel with slices location

## Chapter 2: Computational Methodology

### GOVERNING EQUATIONS

The Navier-Stokes equation is a set of equations that describe the motion of a fluid. The equations can be derived from the basic laws of physics, specifically the laws of conservation of mass, momentum, and energy.

The derivation of the Navier-Stokes equation begins with the Continuity equation, which states that the mass of a fluid within a fixed volume must remain constant over time. This equation is given by:

$$\partial\rho/\partial t + \nabla(\rho.\mathbf{u}) = 0$$

It can be written in the format of;

$$\rho\left(\frac{\partial u}{\partial x} + \frac{\partial v}{\partial y} + \frac{\partial w}{\partial z}\right) = 0$$

Where:

- $\rho$  is the density of the fluid
- $t$  is time
- $\mathbf{u}$  is the velocity vector of the fluid
- $\partial/\partial t$  represents the partial derivative with respect to time
- $\nabla$  represents the gradient operator

Next, the momentum equation is derived. The momentum equation describes the forces that act on a fluid and how they affect its motion. To derive this equation, the principle of conservation of momentum is used, which states that the rate of change of momentum of a fluid within a fixed volume must be equal to the net force acting on the fluid.

The momentum equation for an incompressible fluid is given by:

$$\partial\mathbf{u}/\partial t + (\mathbf{u}.\nabla) \mathbf{u} = -1/\rho.\nabla p + \nu \nabla^2. \mathbf{u}$$

Where:

- $u$  is the velocity vector of the fluid
- $t$  is time
- $p$  is the pressure
- $\rho$  is the density of the fluid
- $\nu$  is the kinematic viscosity
- $\partial/\partial t$  represents the partial derivative with respect to time
- $\nabla$  represents the gradient operator
- $\nabla^2$  represents the Laplacian operator

The left-hand side represents the rate of change of momentum of the fluid and the right-hand side represents the net force acting on the fluid. The first term on the right-hand side represents the pressure gradient force, the second term represents the viscous force, and the last term represents the effect of the change in density due to changes in temperature and pressure.

The Momentum Equation can be derived in a form of,

$$\rho \left( u \frac{\partial u}{\partial x} + v \frac{\partial u}{\partial y} + w \frac{\partial u}{\partial z} \right) = \frac{\partial}{\partial x} \left( \mu \frac{\partial u}{\partial x} \right) + \frac{\partial}{\partial y} \left( \mu \frac{\partial u}{\partial y} \right) + \frac{\partial}{\partial z} \left( \mu \frac{\partial u}{\partial z} \right) - \frac{\partial p}{\partial x}$$

$$\rho \left( u \frac{\partial v}{\partial x} + v \frac{\partial v}{\partial y} + w \frac{\partial v}{\partial z} \right) = \frac{\partial}{\partial x} \left( \mu \frac{\partial v}{\partial x} \right) + \frac{\partial}{\partial y} \left( \mu \frac{\partial v}{\partial y} \right) + \frac{\partial}{\partial z} \left( \mu \frac{\partial v}{\partial z} \right) - \frac{\partial p}{\partial y}$$

$$\rho \left( u \frac{\partial w}{\partial x} + v \frac{\partial w}{\partial y} + w \frac{\partial w}{\partial z} \right) = \frac{\partial}{\partial x} \left( \mu \frac{\partial w}{\partial x} \right) + \frac{\partial}{\partial y} \left( \mu \frac{\partial w}{\partial y} \right) + \frac{\partial}{\partial z} \left( \mu \frac{\partial w}{\partial z} \right) - \frac{\partial p}{\partial z}$$

Finally, the energy equation is derived, also known as the first law of thermodynamics, states that the rate of change of internal energy of a fluid within a fixed volume, plus the work done by the fluid on its surroundings, must be equal to the heat added to the fluid.

$$\rho \left( u \frac{\partial T}{\partial x} + v \frac{\partial T}{\partial y} + w \frac{\partial T}{\partial z} \right) = \frac{\partial}{\partial x} \left( \frac{k_f \partial T}{C_p \partial x} \right) + \frac{\partial}{\partial y} \left( \frac{k_f \partial T}{C_p \partial y} \right) + \frac{\partial}{\partial z} \left( \frac{k_f \partial T}{C_p \partial z} \right)$$

Shortly written as;

$$\partial e / \partial t + \nabla \cdot (e \mathbf{u}) = \nabla \cdot (k \nabla T) + Q$$

Where:

- $e$  is the internal energy per unit mass of the fluid
- $t$  is time
- $\mathbf{u}$  is the velocity vector of the fluid
- $k$  is the thermal conductivity
- $T$  is the temperature
- $Q$  is the heat added to the fluid
- $\partial / \partial t$  represents the partial derivative with respect to time
- $\nabla$  represents the gradient operator

Together, the Continuity equation, the momentum equation, and the energy equation form the Navier-Stokes equations, which describe the motion of a fluid.

The Volume fraction Equation can be derived as;

$$\begin{aligned} \frac{\partial}{\partial x} (\varphi_p \rho_p u_m) + \frac{\partial}{\partial y} (\varphi_p \rho_p v_m) + \frac{\partial}{\partial z} (\varphi_p \rho_p w_m) \\ = - \frac{\partial}{\partial x} [\varphi_p \rho_p u_{dr.p}] - \frac{\partial}{\partial y} [\varphi_p \rho_p v_{dr.p}] - \frac{\partial}{\partial z} [\varphi_p \rho_p w_{dr.p}] \end{aligned}$$

Thermal conductivity can be defined by;

$$k_m = \sum_{s=1}^n \varphi_s k_s$$

Density can be defined by;

$$\rho_m = \sum_{s=1}^n \varphi_s \rho_s$$

Viscosity can be defined by;

$$\mu_m = \sum_{s=1}^n \varphi_s \mu_s$$

$\vec{V}_m$  is mass average velocity and found as:

$$\vec{V}_m = \frac{1}{\rho_m} \sum_{s=1}^n \varphi_s \rho_s \vec{V}_s$$

The drift velocity ( $\vec{V}_{ds,s}$ ) for particles phase (s), i.e. the secondary phase, can be written as:

$$\vec{V}_{ds,s} = \vec{V}_s - \vec{V}_m$$

For the model validation, Launder and Spalding k-ε turbulence model is utilized and expressed by the following equations:

$$\nabla(\rho_m V k) = \nabla \left( \frac{\mu_{t,m}}{\sigma_k} \nabla k \right) + G_m - \rho_m \varepsilon$$

$$\nabla(\rho_m V \varepsilon) = \nabla \left( \frac{\mu_{t,m}}{\sigma_\varepsilon} \nabla \varepsilon \right) + \frac{\varepsilon}{k} (C_1 G_m - C_2 \rho_m \varepsilon)$$

where:

$$\mu_{t,m} = \rho_m C_\mu \frac{K^2}{\varepsilon}, C_1 = 1.44, C_2 = 1.92, C_\mu = 0.09, \sigma_k = 1, \sigma_\varepsilon = 1.3$$

## PERFORMANCE PARAMETERS AND DIMENSIONLESS NUMBERS

There are some parameters that need to be defined in order to perform the study. The Hydraulic Diameter ( $D_h$ ), Reynolds Number, Nusselt Number are one of the major parameters that of the tested channel.

These equations are defined by,

$$\text{Hydraulic Diameter, } D_h = \frac{2WH}{W + H}$$

$$\text{Reynolds Number, } Re = \frac{\rho_{in} w_{in} D_h}{\mu_{in}}$$

$$\text{Nusselt Number , } Nu_{avg} = \frac{HD_h}{k_f}$$

Friction factor can be obtained by the following equation;

$$f = \frac{2\Delta p D_h}{\rho_f w_{in}^2 L_{cor}}$$

The enhancement ratio, i.e., performance parameter related to heat transfer, is defined as:

$$\text{Enhancement ratio} = \frac{Nu_{av,mod}}{Nu_{av,ref}}$$

In order to test the modified system which consists of curved corrugated channel with and without baffles for both water and nanofluids against a base system which including smooth channel with water, the thermal -hydraulic performance factor (THPF) is adopted as:

$$THPF = \frac{Nu_{av,ref}}{Nu_{av,mod}} \left( \frac{f_{mod}}{f_{ref}} \right)^{\sqrt{3}}$$

For determining the thermophysical characteristics of fluids, the bulk mean temperature of the fluid ( $T_m$ ) is considered;

$$T_m = \frac{T_{in} + T_{out}}{2}$$

Calculating the heat transferred to the fluid through the corrugated pipe,

$$\dot{Q} = mc_p(T_{out} - T_{in})$$

The heat Transfer coefficient can be gained from;

$$\dot{Q} = hA_c\Delta T_c \quad \rightarrow \quad h = \frac{\dot{Q}}{A_c\Delta T_c}$$

## **NUMERICAL IMPLEMENTATION**

A commercial computational fluid dynamics software, ANSYS-FLUENT V19.R2, was employed to simulate and solve the governing equations and boundary conditions for their study. The finite volume method was used for the discretization of the equations. The SIMPLE scheme was applied for the pressure-velocity coupling and the second-order upwind scheme was used to solve the momentum and energy equations. A standard wall function with a standard k- $\epsilon$  model was also utilized in the analysis. The simulations were run until a convergence criterion of  $10^{-6}$  for the flow equations and  $10^{-6}$  for the energy equation was met, on average this took 1000 iterations and 35 minutes using Acer Computer with Intel(R) Core (TM) i5-8400 CPU 2.80GHz.

## **MESH GENERATION AND GRID INDEPENDENCE ANALYSIS**

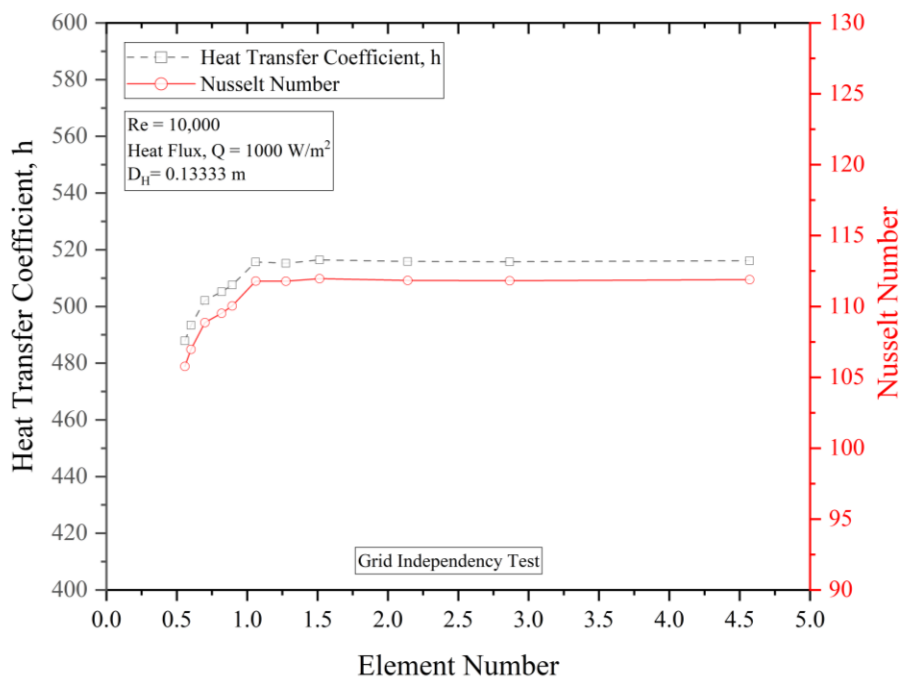
The method of solving the governing equations and applying the appropriate boundary conditions is used to perform calculations for the complex flow problem under examination. ANSYS-FLUENT-V19.R2, which is based on the finite volume method, is employed to simulate the fluid flow and discretize the governing equations. The standard k- $\epsilon$  turbulence model, which is commonly used for fully turbulent flow, is utilized in this simulation to accurately depict the current complex flow. Many researchers have used this method to simulate turbulent flow in corrugated channels/baffled channels and have found a good correlation between the numerical results obtained by the k- $\epsilon$  model and experimental data.

To better understand the flow characteristics in pipes, a steady state and three-dimensional model is created to generate a computational domain that includes baffles and corrugations in the pipe. The development of grid domains is a crucial phase in the numerical calculations as it affects both computation time and accuracy. The complex flow behavior near the surface of baffles and corrugated pipes greatly influences the pressure drop and Nu number. The flow generation region is critical to the mesh's computational efficiency as well as its accuracy outcomes.

A fine mesh is employed along the wall and a rather coarse mesh is used near the centerline to improve the convergence results. The computational flow domains are discretized using a structured-tetrahedral mesh, which is known for its ability to provide more accurate flow

calculations. The use of inflation layers also helps to ensure accurate computations. Several meshes are evaluated to assess how numerical results are affected. Figure 2 shows a section plane along the radial direction of the curved corrugated pipe to provide a visual representation of the mesh.

The grid independence studies are performed before simulations to determine the appropriate mesh size with the lowest feasible time consumption. To ensure accuracy, grid independent methods are obtained by conducting thorough mesh testing procedures. The corrugated pipe geometry is examined using various grid element counts. Nu, velocity, and pressure drop are all taken into consideration with different element numbers to determine if there are any significant variations with respect to the element numbers. In this study, multiple grid generations are carried out when the number of mesh elements ranges from 0.5 million to 4.6 million. The flow mesh features for the dimple pipe. It is determined that approximately 1.51 million elements achieve mesh-independent convergence.



Graph 1: Nusselt Number variation with change of Mesh elements

Obtaining the optimal mesh size takes both pressures drop and Nusselt number into account. Increasing the range of elements above 1.51 million is unlikely to affect pressure drop and



Nusselt number. The  $y^+$  value, which is the non-dimensionalized near-wall grid spacing using shear stress velocity, is used to define how coarse or fine a mesh is for a specific flow regime. To accurately represent the turbulence modeling, it is essential to find the optimal cell size close to domain edges. In terms of saving time and reducing computing expenses, this number of elements is chosen for analysis.

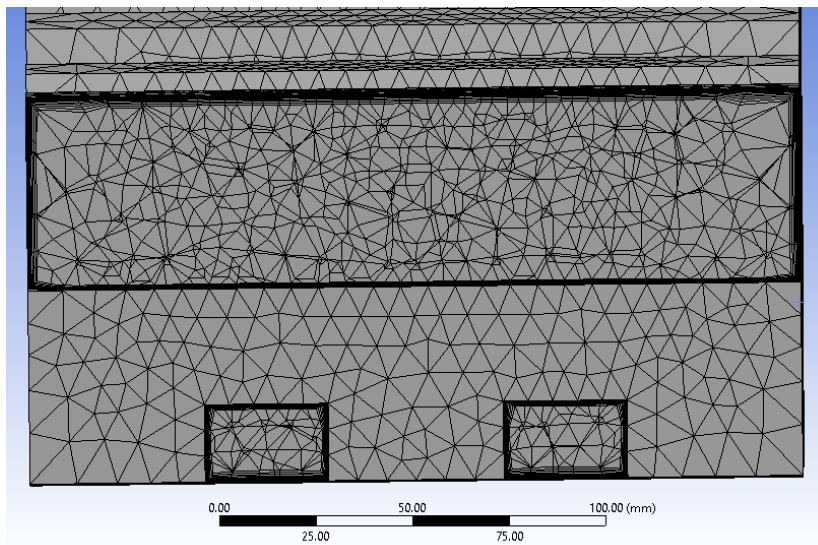
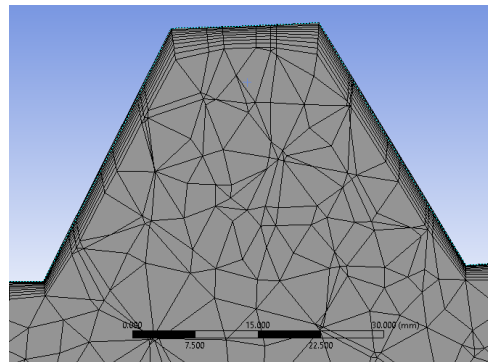
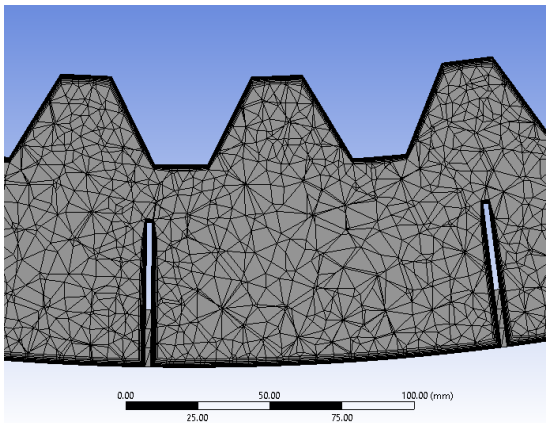
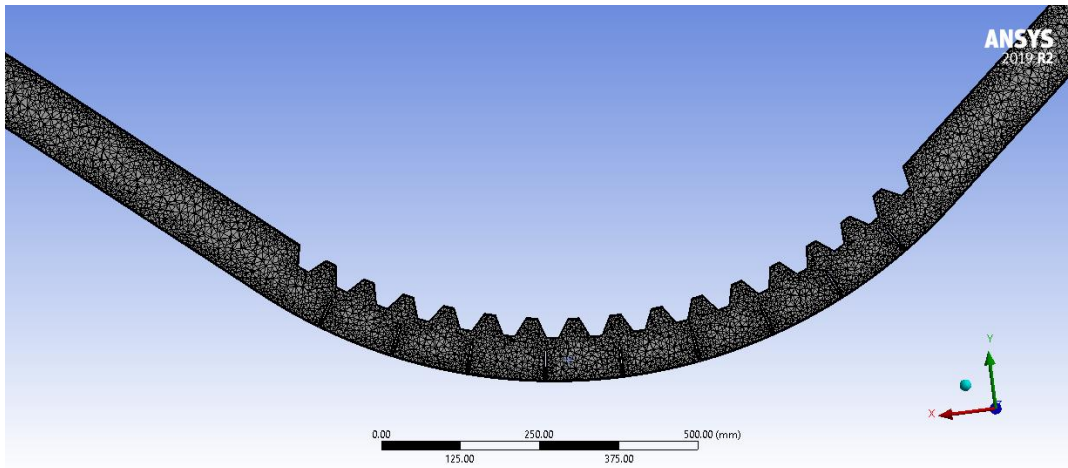


Figure 2: Different views of mesh with inflation layer.

## CODE VALIDATION

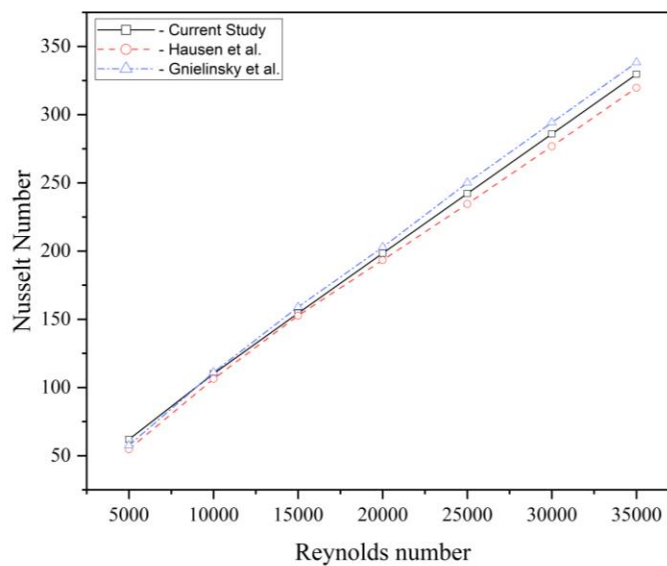
For numerical simulation of turbulent flow in a pipe, it is necessary to validate the accuracy of the current numerical results. An experimental validation of heat transfer performance should be accomplished first to evaluate the numerical system's reliability for flow, pressure drop, and heat performance. The numerical results for the corrugated tubes are in agreement with the data, as shown in the figure. The computational model was tested against available experimental data, and some correlations were found as indicated in the following equation. Eqs. (1) and (2) were used to calculate the Nusselt number of water and the friction factor of water, respectively, for validation. The equation was given by Hausen et al.;

$$Nu = 0.037(Re^{0.75} - 180)Pr^{0.42} \left[ 1 + \left( \frac{2h}{x} \right)^{\frac{2}{3}} \right]$$

Where X is the entry length.

Hausen's equation was further refined by Gnielinsky for higher Prandtl number.

$$Nu = 0.012(Re^{0.87} - 180)Pr^{0.4} \left[ 1 + \left( \frac{2h}{x} \right)^{\frac{2}{3}} \right]$$



Graph 2: Model Validation

The Nusselt number and computational outcomes appear to be in good agreement when compared numerically. Because of this, it can be argued that the existing computational model can accurately forecast the flow and thermal performance of the pipe.

## THERMOPHYSICAL PROPERTIES OF NANOFLUIDS

In order to conduct the study, the usage of nanofluid is essential. Recently, numerous research studies have been conducted to develop strategies for calculating the thermophysical properties of nanofluids. Due to their favorable thermophysical characteristics, the use of nanofluids in cooling applications has increased. Despite the extensive research on the thermophysical characteristics of nanofluids, the experimental data is often controversial and lacks precision. A single-phase technique is commonly used in the literature for measuring thermophysical parameters. This approach assumes that the correlation of convective heat transfer can also be applied if the nanofluid properties and the thermophysical property estimated at reference temperatures are taken into account [30–32]. According to the model presented by Maga et al. [33], nanofluids with oxide particles larger than 40 nm should be given priority. The effective properties of nanofluids are determined using the following equations.

The density of nanofluids is derived using;

$$\rho_{nf} = (1 - \phi)\rho_{bf} + \phi\rho_s$$

The correlation provided by Takabi and Salehi [34] based on the rule of mixtures was used to define the density of hybrid nanofluids;

$$\rho_{hnf} = (1 - \phi)\rho_{bf} + \phi_{s,1}\rho_1 + \phi_{s,2}\rho_2$$

Where;

- $\phi_{s,1}$  = volume fractions of 1st nanoparticle in the base fluid
- $\phi_{s,2}$  = volume fractions of 2nd nanoparticle in the base fluid
- $\rho_1$  = 1st nanoparticle density
- $\rho_2$  = 2nd nanoparticle density

The volume fraction ( $\phi$ ) of nanofluid is added as a new variable;

$$\phi = \frac{V_s}{V_{bf}}$$

Furthermore, the volume fractions of each sort of nanoparticles are specified as follows:

$$\phi_{s,1} = \frac{V_{s,1}}{V_{bf}} \quad \phi_{s,2} = \frac{V_{s,2}}{V_{bf}}$$

Nanofluid specific heat capacity is determined by comparing the density, volume fraction and specific heat capacities of the base fluid and nanoparticles [35];

$$C_{p,nf}\rho_{nf} = (1 - \phi)C_{p,bf}\rho_{bf} + \phi C_{p,s}\rho_s$$

The equation below was used to calculate the hybrid nanofluid's specific heat capacity [[34]];

$$C_{p,hnf} = \frac{(1 - \phi)C_{p,bf}\rho_{bf} + \phi_{s,1}\rho_1 C_{p,1} + \phi_{s,2}\rho_2 C_{p,2}}{\rho_{hnf}}$$

According to the Brinkman equation, the dynamic viscosity of nanofluids can be computed as follows [36];

$$\mu_{nf} = \frac{\mu_{bf}}{(1 - \phi)^{2.5}}$$

Regarding hybrid nanofluids, the volume fraction of both nanoparticles in the base fluid has been computed as follows using a modified version of the Brinkman equation [37];

$$\mu_{hnf} = \frac{\mu_{bf}}{(1 - \phi_{s,1})^{2.5} + (1 - \phi_{s,2})^{2.5}}$$

The thermal conductivity of nanofluids is determined utilizing the Hamilton–Crosser model, a modified version of Maxwell's theory.

$$k_{nf} = k_{bf} \frac{k_s + (n - 1)k_{bf} - \varphi(n - 1)(k_{bf} - k_s)}{k_s + (n - 1)k_{bf} + \varphi(k_{bf} - k_s)}$$

Where  $n = \frac{3}{\psi}$  and  $\psi$  denotes the sphericity of the particles.

**Table 3**

Properties of base fluid and nanoparticles [38–40]

Material	Density, $\rho$ (kg/ m <sup>3</sup> )	Heat capacity, Cp (J/kgK)	Thermal conductivity K (W/mK)	Dynamic viscosity, $\mu$ (kg/ms) $\times 10^{-3}$
Al <sub>2</sub> O <sub>3</sub>	3970	765	40.0	–
CuO	6510	540	18.0	–
TiO <sub>2</sub>	4250	686	8.945	–
ZnO	5600	495.2	13	–

**Table 4**Thermophysical properties of water-based nanofluids for  $\phi = 1\%$  [38,39]

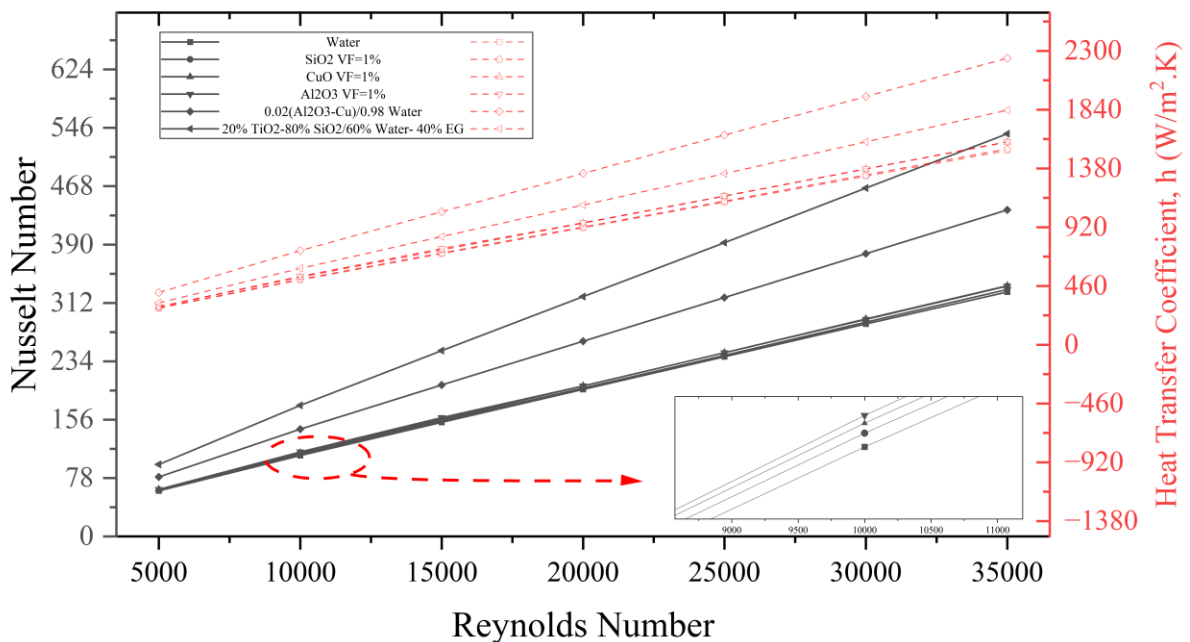
Thermo-physical properties	Al <sub>2</sub> O <sub>3</sub>	CuO	TiO <sub>2</sub>	ZnO	Al <sub>2</sub> O <sub>3</sub> - TiO <sub>2</sub>
Density	1023.129	1049.15	1028.24	1087.35	1011.74
Heat capacity	4058.87	3953.75	4033.68	3807.7	4106.58
Thermal conductivity	0.630	0.629	0.630	0.672	0.623
Dynamic viscosity	9.14	9.14	9.14	9.14	9.14

# Chapter 3: Result and Discussion

## RESULT AND DISCUSSION

### Effect of Nanofluid

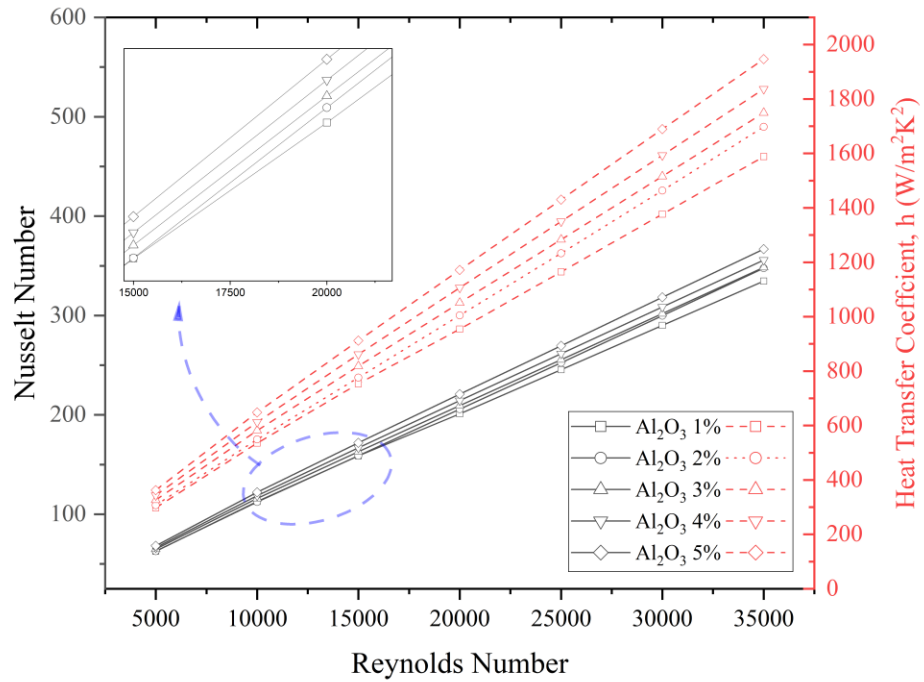
The use of nanofluids in curved corrugated pipes can have several effects on fluid flow and heat transfer. Nanofluids are a type of engineered fluid in which nanoparticles are dispersed in a base fluid, such as water or oil. The presence of nanoparticles alters the properties of the base fluid and can lead to enhanced heat transfer characteristics.



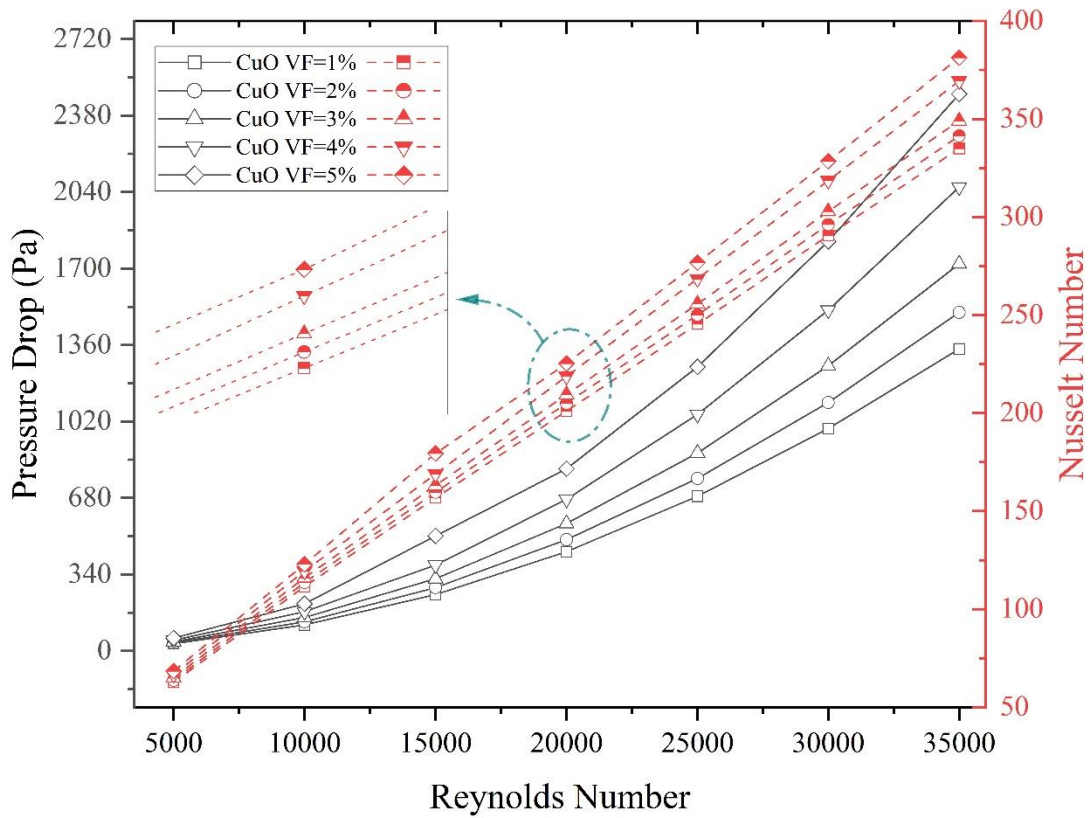
Graph 3: Deviation of Nusselt Number and Heat transfer Coefficient for different nanofluid and Hybrid Nanofluid

Here we can see the increment of heat transfer de to the change of nanofluid. Hybrid nanofluid has been used in order to increase the heat transfer coefficient leading to an increment in Nusselt Number.





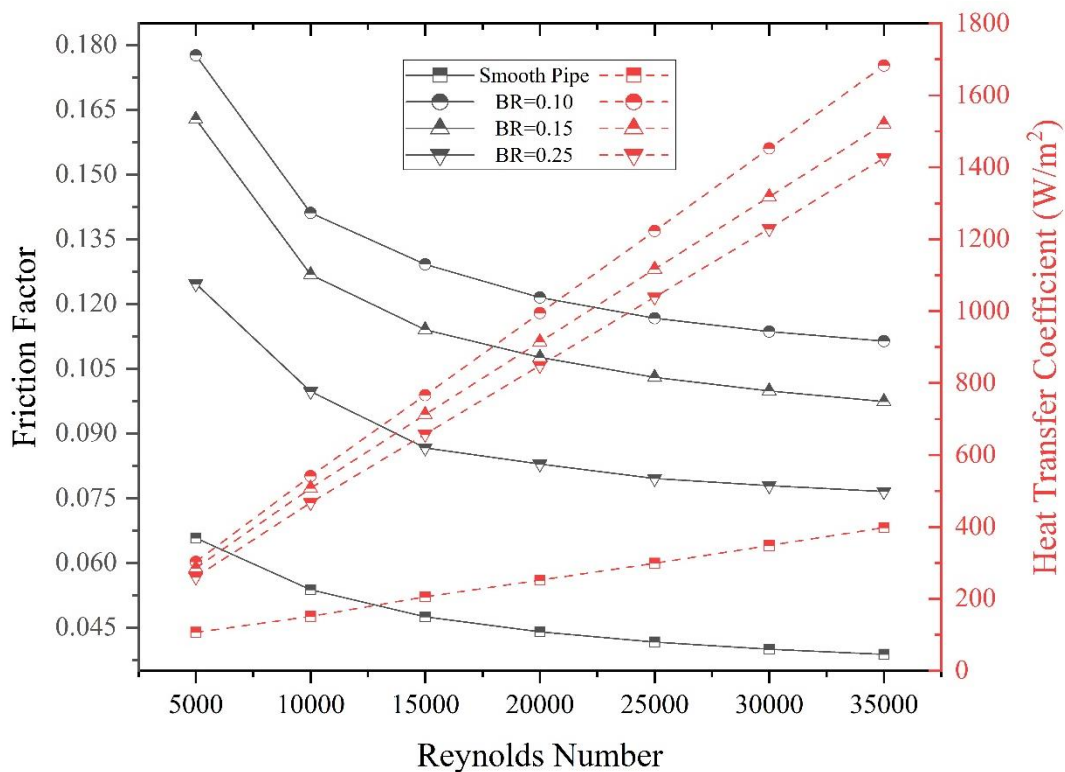
Graph 4: Deviation of Nusselt Number and Heat transfer Coefficient for different Volume Fraction of  $Al_2O_3$



Graph 4: Deviation of Nusselt Number and Pressure Drop for different Volume Fraction of CuO

## Effect of blockage ratio

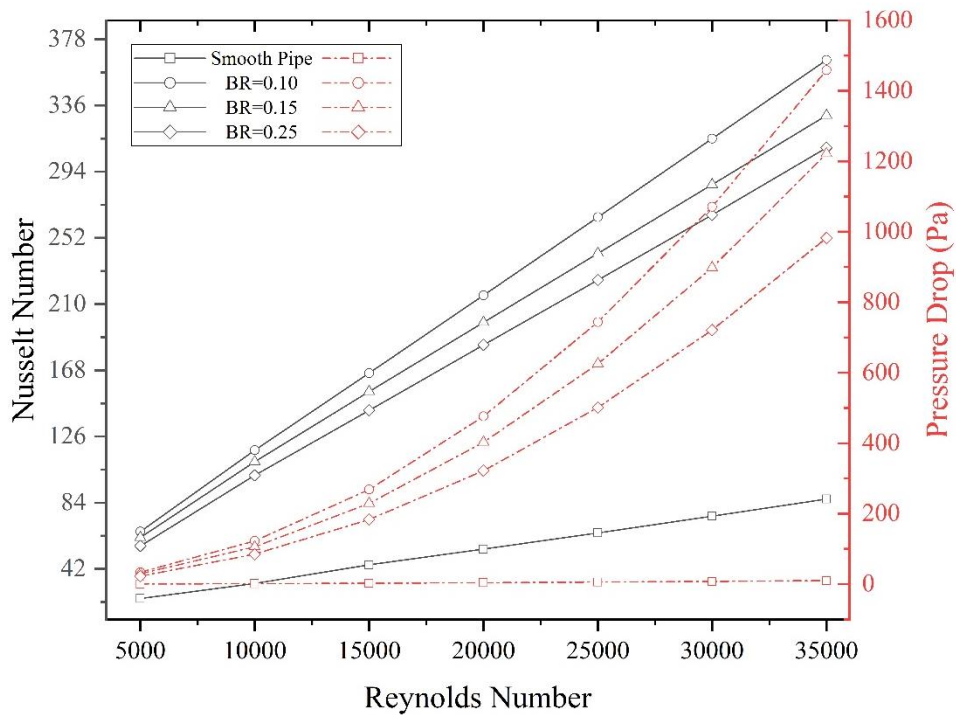
In this section, the baffled curved-corrugated channel with inline manner is discussed and analyzed at different blockage ratio (BR = 0.10, 0.15 and 0.25) and different volume fraction of ZnO-water nanofluid at  $\beta=10^\circ$  and GR = 0.2 over Re 5000–35,000. Figure demonstrates the distributions in slice planes of the tested channel at BR = 0.10, 0.15 and 0.25, respectively. In general, The Nusselt Number distribution in the baffled curved-corrugated channel is affected sharply by the vortex shedding from the corrugations and baffles along the walls of channel.



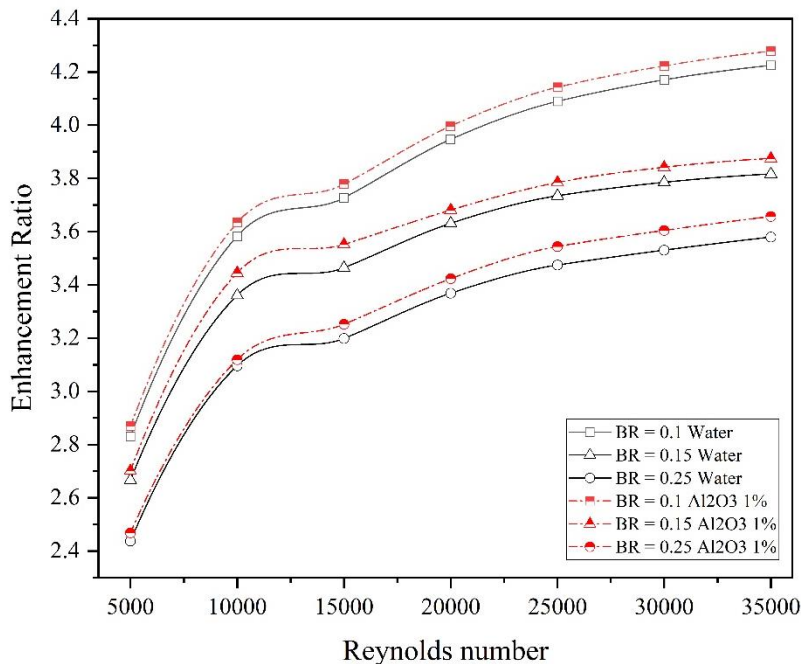
Graph 5: Deviation of Friction Factor and heat transfer coefficient for Different Blockage Ratio

As observed, the area with the smaller shear stress for BR = 0.2 is comparatively smaller than that of other cases in the slices of the channel studied, which is stemmed from the fact that the velocity in the viscous sub-layer is declined at a small value of BR. In addition, it is noted for all cases that due to the interaction between fluid motion and baffle, the majority of zone with high value of

shear stress was found close the baffle structure. After the baffle, the shear stress is little by little decreased along the streamwise and turn out to be smaller due to the reduction of walls restriction. When the BR rises, the vortex shedding from the baffles is slowly intensified, interacting with the other vortex from the corresponding baffle and the upper vortex from corrugations, and impelling higher velocity fluid through a viscous sub-layer, continuously colliding with the channel walls.



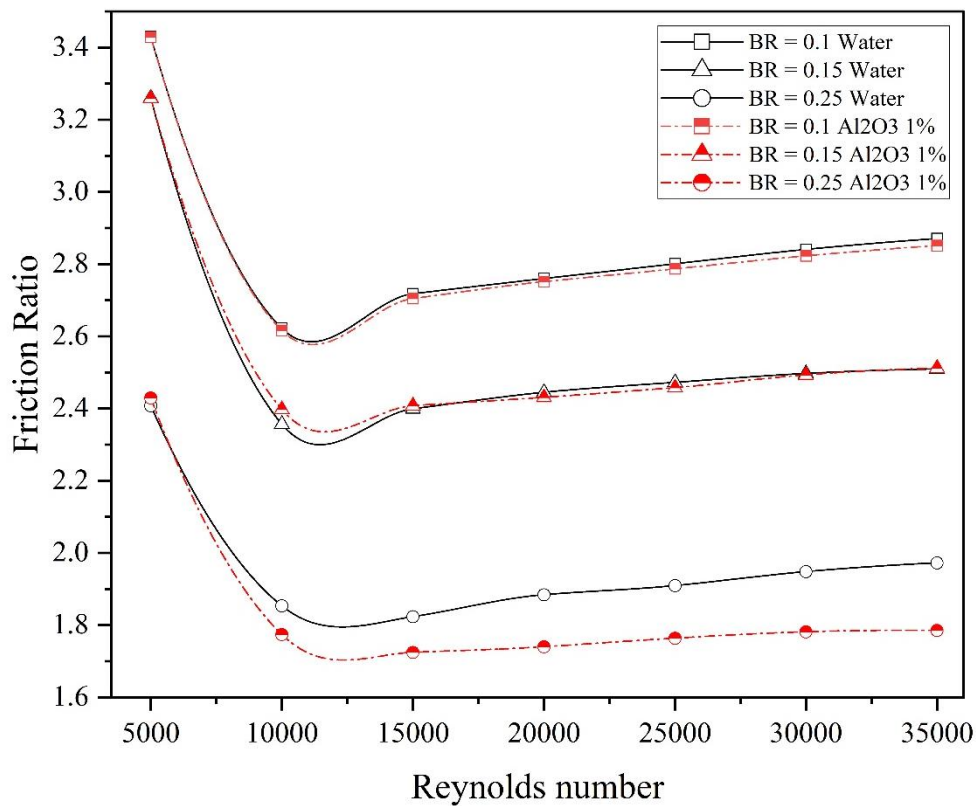
Graph 6: Deviation of Nusselt Number and Pressure Drop for Different Blockage Ratio



we can observe that as the Reynolds number increases, the enhancement ratio also increases. This means that the modification applied to the pipe is becoming more effective at higher Reynolds numbers.

An increasing enhancement ratio suggests that the modification technique used in the modified model improves the convective heat transfer compared to the reference model. The modification may introduce additional turbulence, increase surface area, or enhance fluid mixing, resulting in improved heat transfer. As the Reynolds number increases, the flow becomes more turbulent, and the modification becomes more efficient in enhancing heat transfer.

It is important to note that the specific details of the modification technique and the experimental setup can influence the observed trends. However, based on the given data, we can conclude that increasing the Reynolds number is associated with an increasing enhancement ratio, indicating improved convective heat transfer in the modified model compared to the reference model



The friction ratio in a curved corrugated pipe refers to the ratio of the friction factor ( $f$ ) of the pipe with corrugations to the friction factor of a smooth pipe ( $f_0$ ) under similar flow conditions. The friction factor is a dimensionless parameter that quantifies the resistance to flow in a pipe.

From your experiment, you have observed that the friction ratio initially decreases as the Reynolds number increases and then starts to increase. This behavior can be explained by considering the influence of two key factors: the flow regime and the geometry of the curved corrugated pipe. At low Reynolds numbers, the flow in the curved corrugated pipe is typically laminar, with smooth and predictable streamlines. In this regime, the friction ratio decreases because the corrugations disturb the flow less than in a straight pipe, resulting in reduced frictional losses. The irregularities on the pipe's surface can act as secondary flow generators, promoting better flow mixing and reduced boundary layer growth.

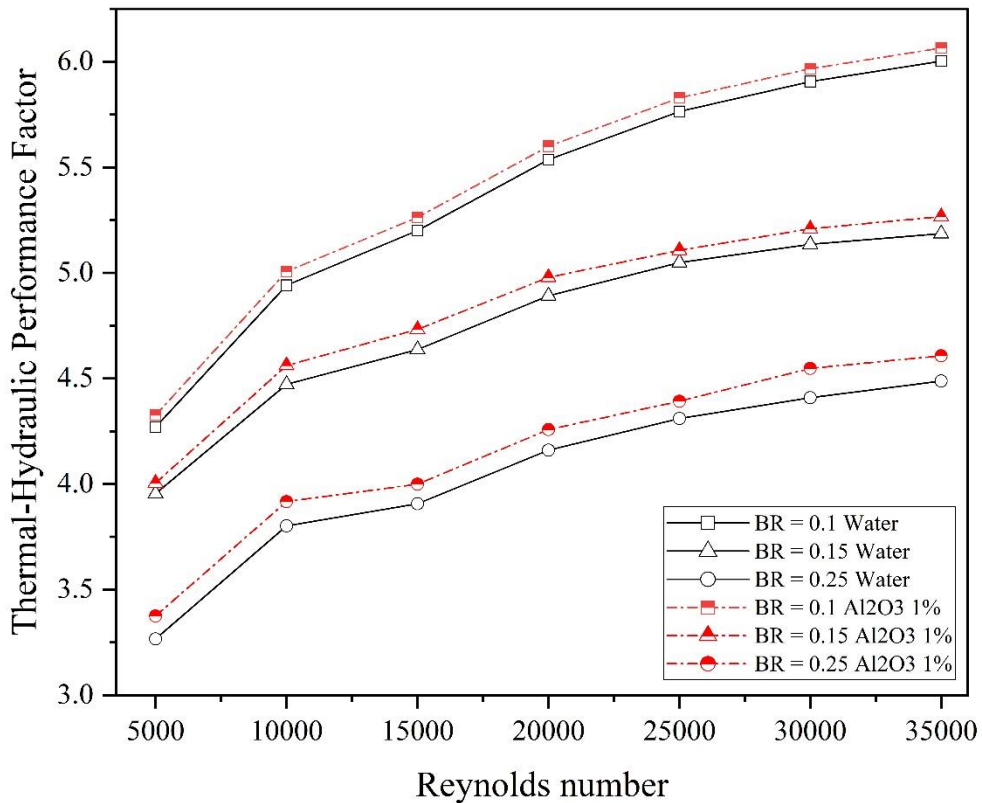
As the Reynolds number increases, the flow transitions from laminar to transitional and eventually to turbulent. In the transitional and turbulent flow regimes, the flow becomes more chaotic and the interaction between the fluid and the corrugations intensifies. This leads to increased frictional losses compared to laminar flow, causing the friction ratio to start increasing.

The Thermal Hydraulic Performance Factor (THPF) in a curved corrugated pipe refers to a dimensionless parameter that characterizes the combined heat transfer and pressure drop performance of the pipe. It is typically defined as the ratio of the Nusselt number ( $Nu$ ) to the friction factor ( $f$ ) raised to the power of a specific exponent, often denoted as  $m$ . The THPF is given by the equation:  $THPF = Nu / (f^m)$ .

Based on your experiment, you have observed that the THPF increases as the Reynolds number increases. This behavior can be explained by considering the influence of the Reynolds number on both heat transfer and pressure drop characteristics in a curved corrugated pipe.

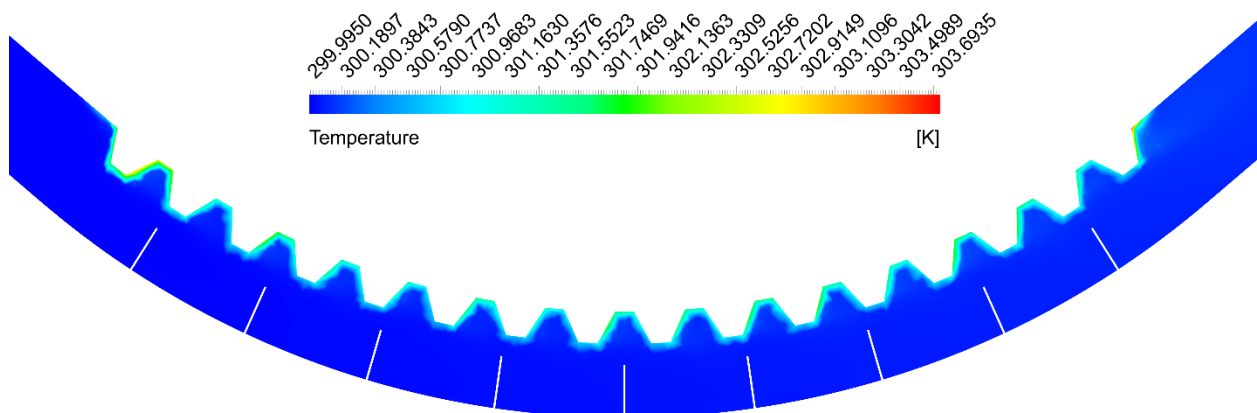
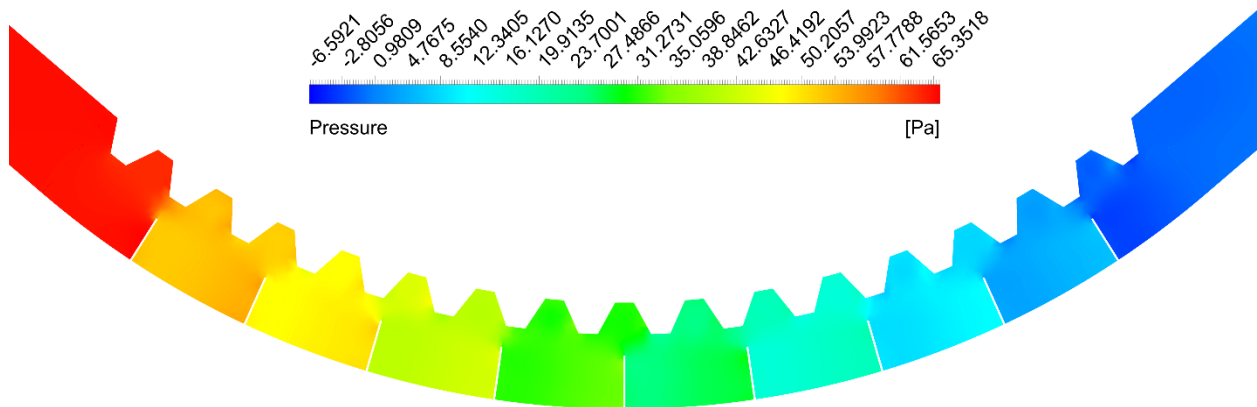
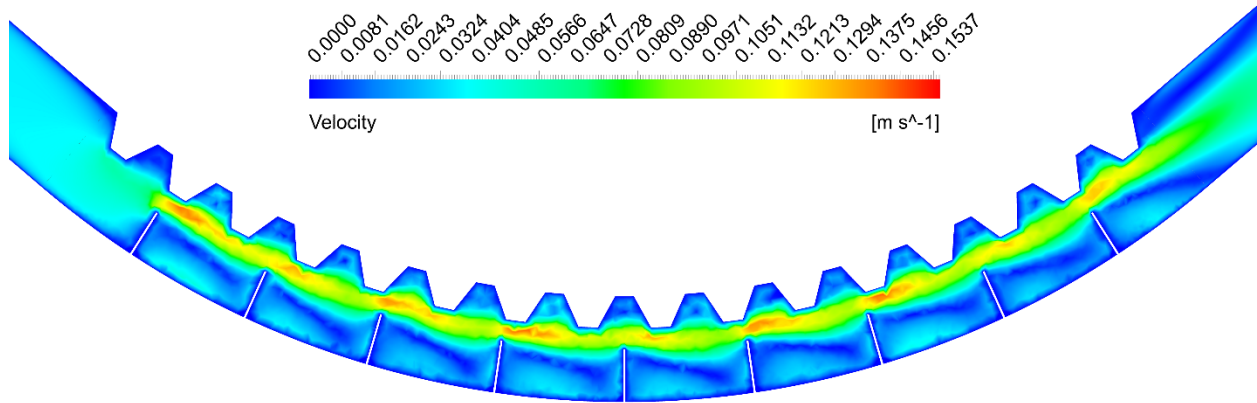
As the Reynolds number increases, the flow in the curved corrugated pipe transitions from laminar to transitional and eventually to turbulent. Turbulent flow is known to promote better heat transfer due to increased fluid mixing and enhanced turbulence-induced convective heat transfer. The increased Reynolds number leads to increased turbulence levels, which can result in higher Nusselt numbers ( $Nu$ ) and improved heat transfer performance.

In a curved corrugated pipe, the presence of corrugations further enhances the heat transfer due to increased surface area and disruption of the thermal boundary layer. The irregularities on the pipe's surface induce secondary flows, which help in better mixing and heat transfer between the fluid and the pipe walls. The increased Reynolds number intensifies these effects, leading to higher heat transfer coefficients and, consequently, a higher Nusselt number.

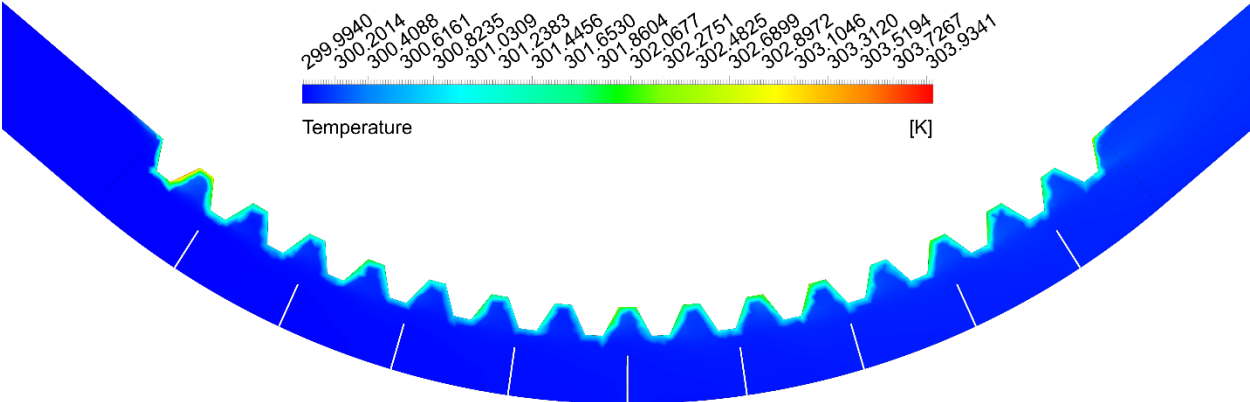
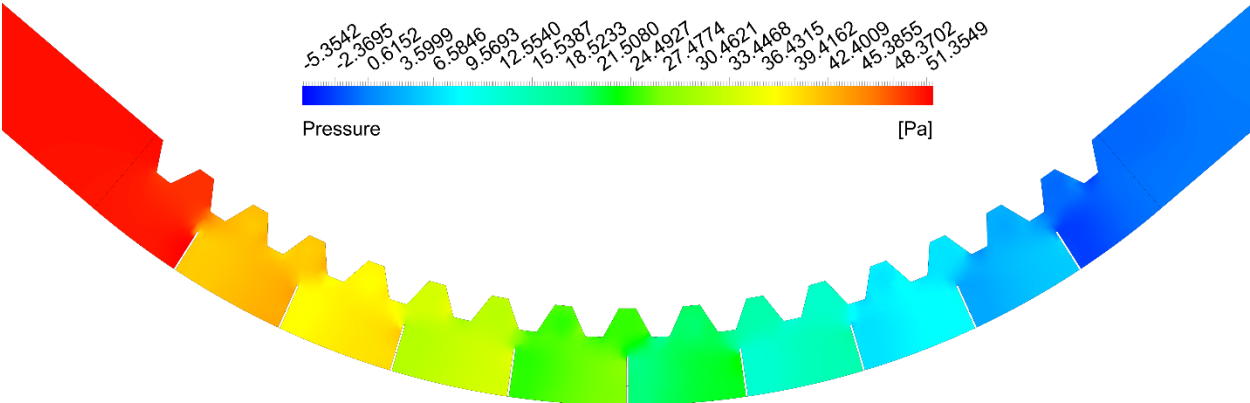
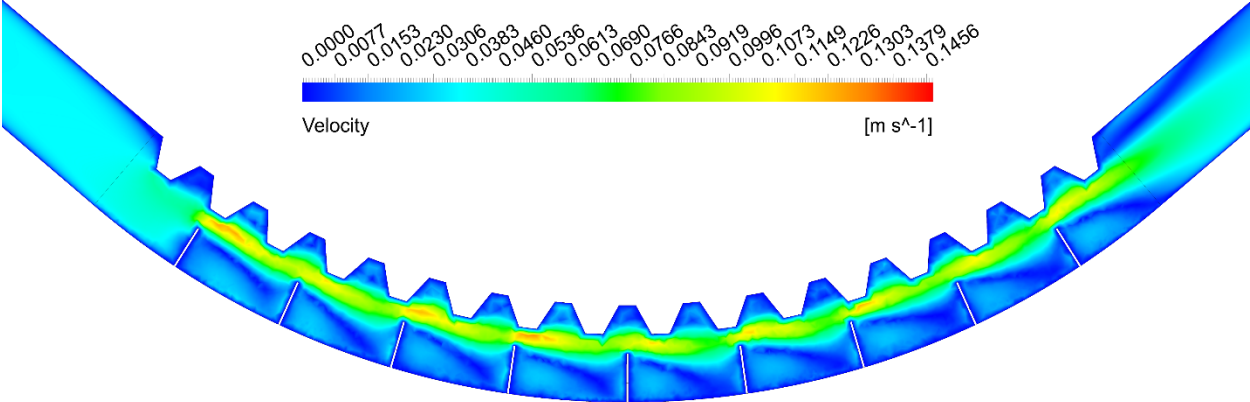


# FLOW BEHAVIOR INVESTIGATIONS

For a BR of 0.15 the flow characteristic is having below;

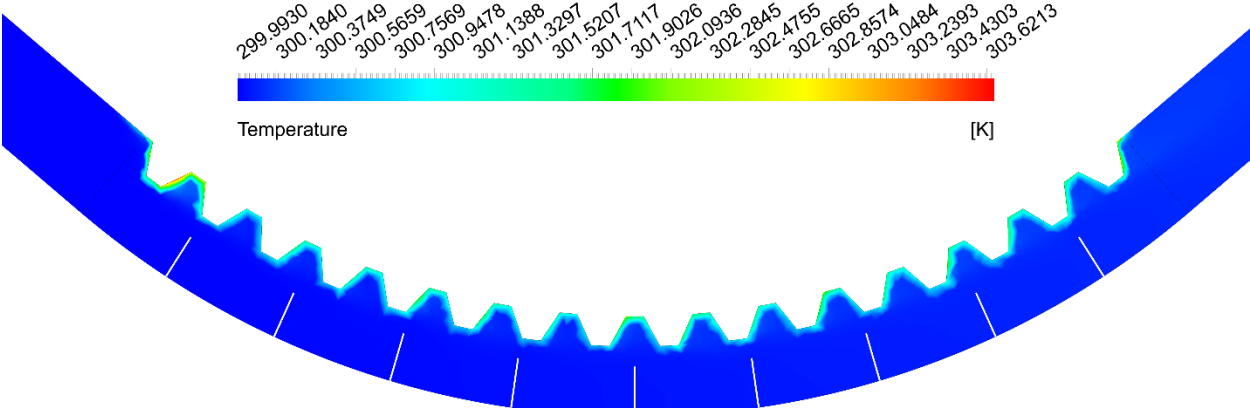
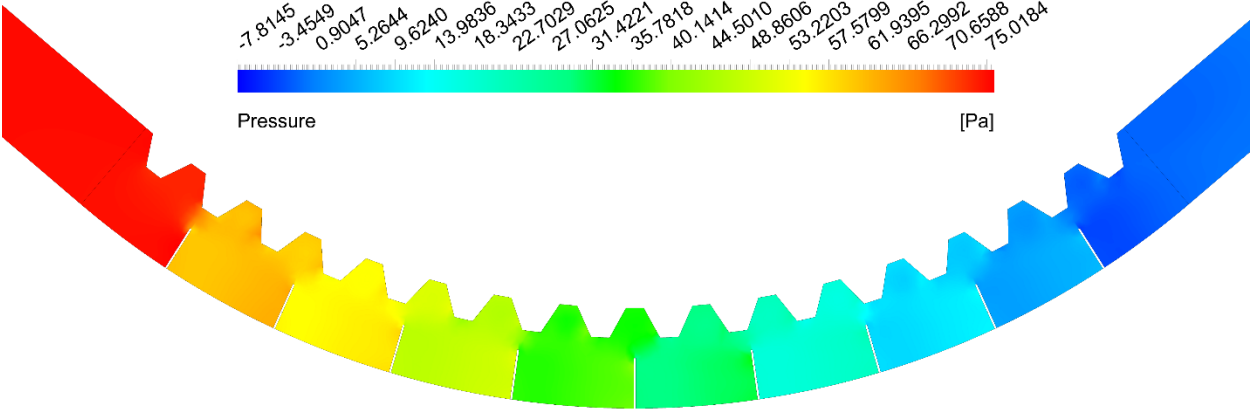
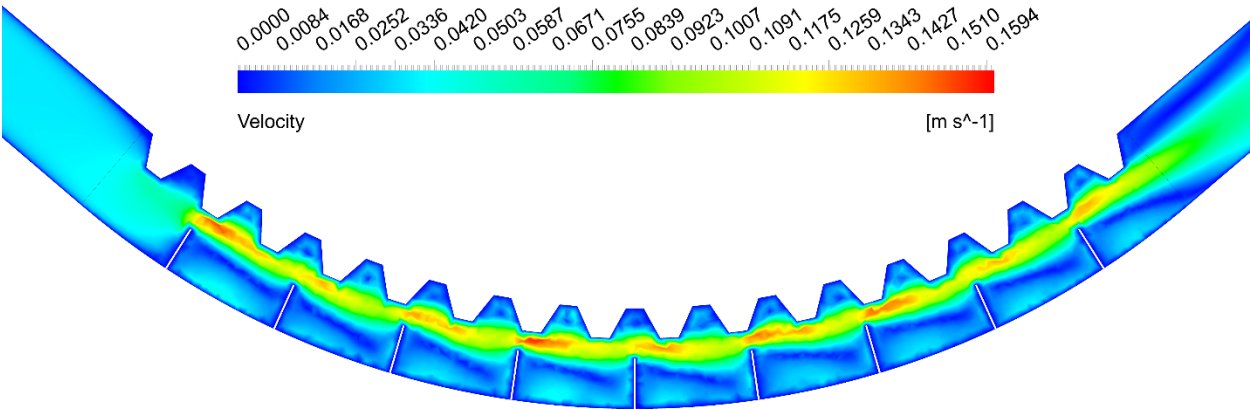


For a BR of 0.10 the flow characteristic is having below;





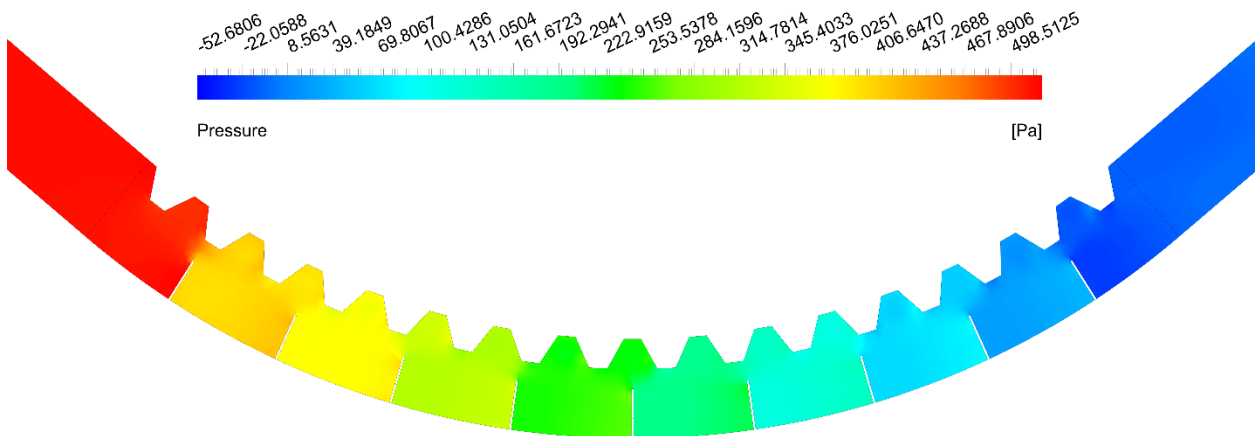
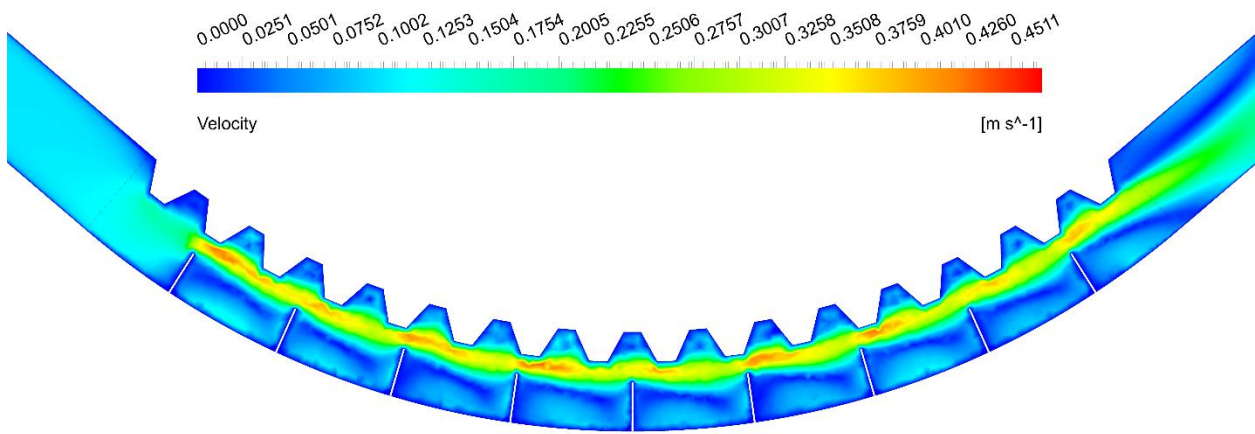
For a BR of 0.25 the flow characteristic is having below;



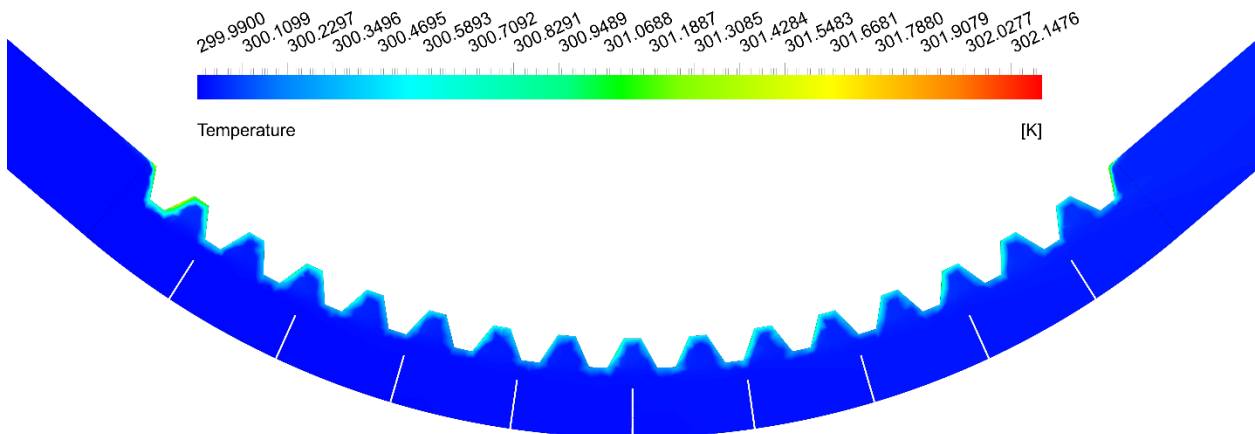
Due to the increment of the Reynolds Number the flow condition can change as follow;

Reynolds Number = 15000

**ANSYS**  
2019 R2

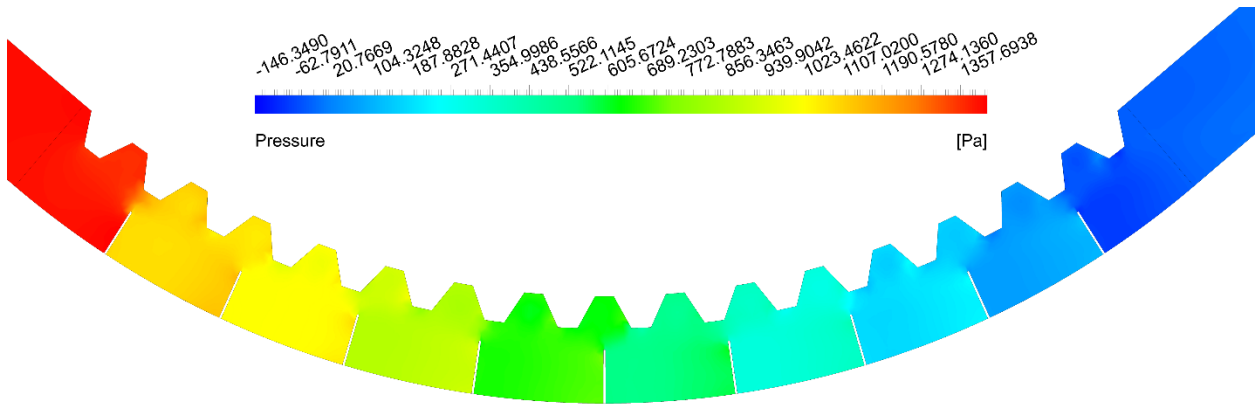
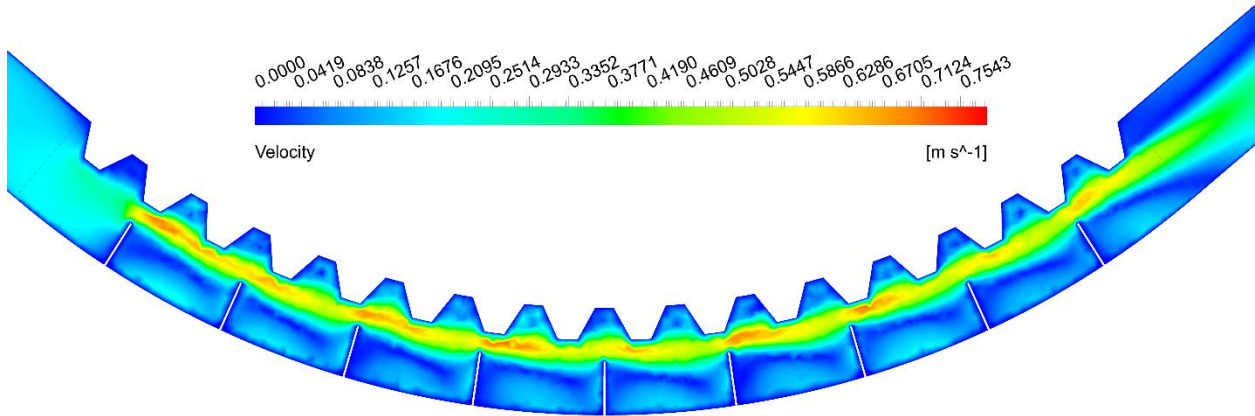


**ANSYS**  
2019 R2

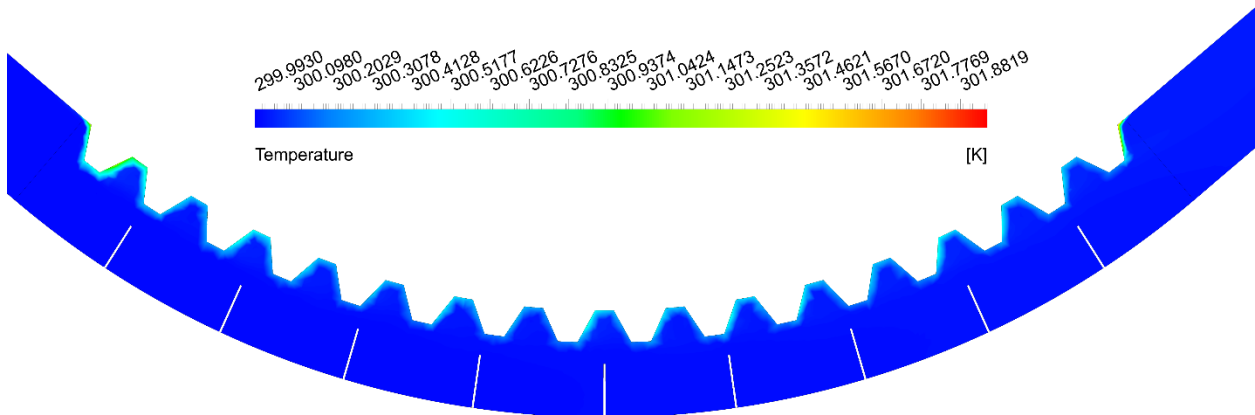


Reynolds Number = 25000

**ANSYS**  
2019 R2

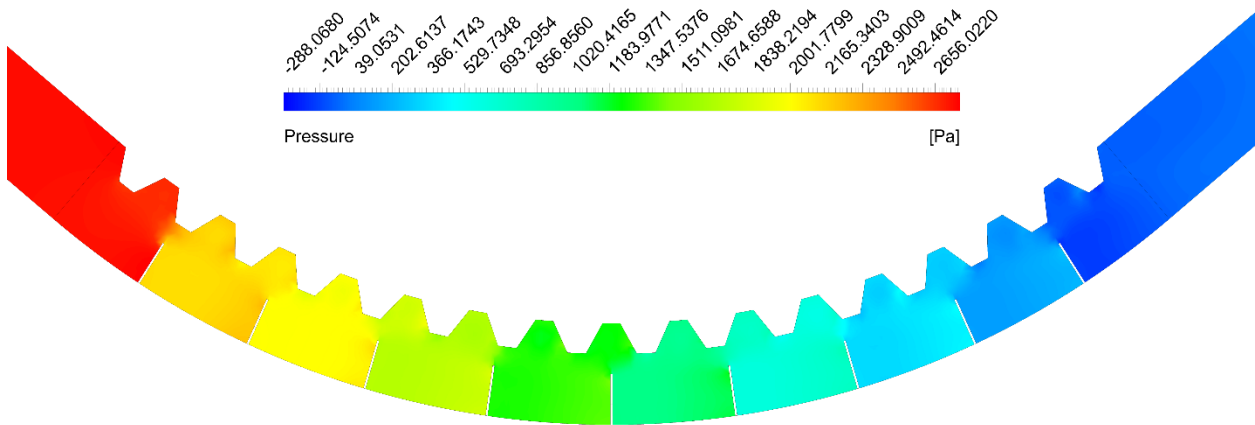
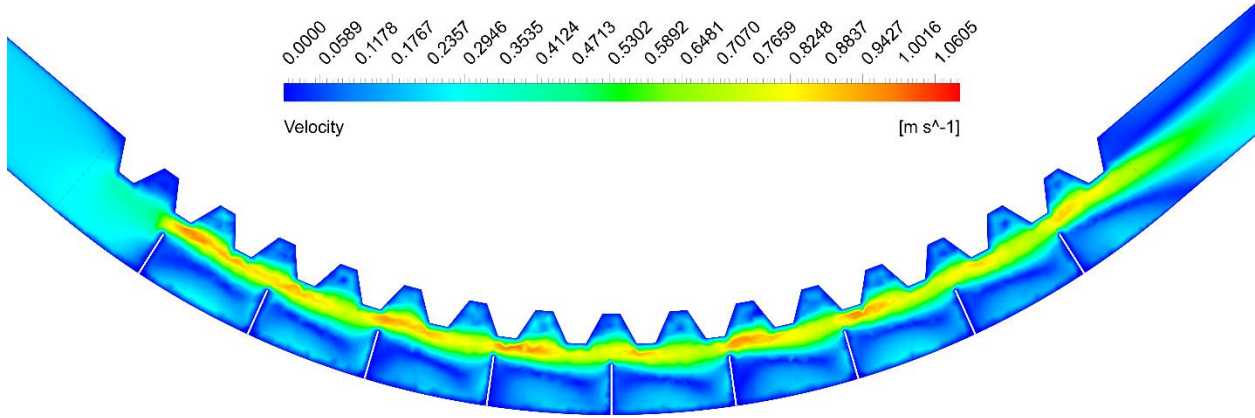


**ANSYS**  
2019 R2

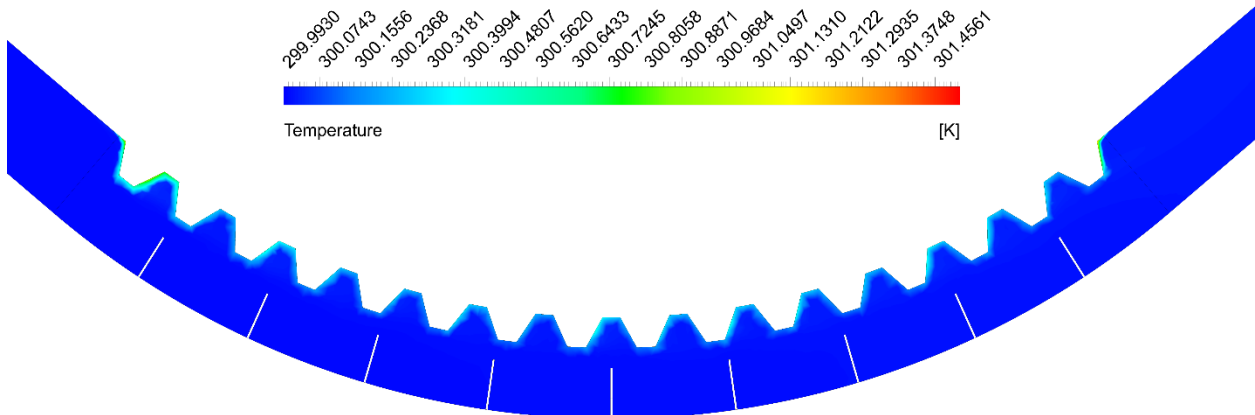


Reynolds Number = 35000

**ANSYS**  
2019 R2



**ANSYS**  
2019 R2



## Chapter 4: Conclusion

In this study, curved model with corrugation has been analyzed for the heat transfer enhancement criteria. Due to the presence of corrugation and baffles, it has its own unique characteristics to improve the heat transfer rate.

The aim of this research is to determine whether particular geometric patterns on a corrugated tube with the use of hybrid nanofluids, can lead to improved heat transfer characteristics or not.

For the corrugated channel with baffles, it is found out that the Nusselt no for nanofluid is greater than that of water. In comparison to a straight pipe, the performance of a corrugated pipe with baffles has better output for getting the optimal thermal performance. Due to the creation of recirculation areas, higher velocity and higher turbulent energy can be achieved. Optimizing the shape of corrugated pipes with more intricate geometric design will result in more efficient heat conductors.

Besides, by further changing the design of corrugated section or the baffles, the heat transfer rate can be changed. By incorporating nanofluid as the working fluid, the chances of getting higher heat transfer coefficient will increase. The more complex design of geometry, the greater value of pressure-drop and Nu no. As the Re number (a dimensionless number used to describe the ratio of inertial forces to viscous forces) for geometric patterns on corrugated pipes approaches its peak value, the enhancement of the Nu number also tends to increase.

As the proportion of each nanofluid in the mixture is increased, the volumetric entropy generation decreases which is a good sign for heat transfer enhancement. So, by changing the volume fraction of different nanofluids, the change in heat transfer rate can be observed for this particular geometry.

## Chapter 5: References

- [1] P. Promvonge, S. Skullong, S. Kwankaomeng, C. Thiangpong, Heat transfer in square duct fitted diagonally with angle-finned tape-Part 2: Numerical study, *International Communications in Heat and Mass Transfer*. 39 (2012) 625–633. <https://doi.org/10.1016/j.icheatmasstransfer.2012.03.010>.
- [2] P. Promvonge, S. Tamna, M. Pimsarn, C. Thianpong, Thermal characterization in a circular tube fitted with inclined horseshoe baffles, *Appl Therm Eng*. 75 (2015) 1147–1155. <https://doi.org/10.1016/j.applthermaleng.2014.10.045>.
- [3] D. Sahel, H. Ameer, R. Benzeguir, Y. Kamla, Enhancement of heat transfer in a rectangular channel with perforated baffles, *Appl Therm Eng*. 101 (2016) 156–164. <https://doi.org/10.1016/j.applthermaleng.2016.02.136>.
- [4] A. Khanlari, H.Ö. Güler, A.D. Tuncer, C. Şirin, Y.C. Bilge, Y. Yılmaz, A. Güngör, Experimental and numerical study of the effect of integrating plus-shaped perforated baffles to solar air collector in drying application, *Renew Energy*. 145 (2020) 1677–1692. <https://doi.org/10.1016/j.renene.2019.07.076>.
- [5] J.J. Fiuk, K. Dutkowski, Experimental investigations on thermal efficiency of a prototype passive solar air collector with wavelike baffles, *Solar Energy*. 188 (2019) 495–506. <https://doi.org/10.1016/j.solener.2019.06.030>.
- [6] J. Cabonce, R. Fernando, H. Wang, H. Chanson, Using small triangular baffles to facilitate upstream fish passage in standard box culverts, *Environmental Fluid Mechanics*. 19 (2019) 157–179. <https://doi.org/10.1007/s10652-018-9604-x>.
- [7] Y. Wang, K.C. Smith, Numerical investigation of convective transport in redox flow battery tanks: Using baffles to increase utilization, *J Energy Storage*. 25 (2019). <https://doi.org/10.1016/j.est.2019.100840>.
- [8] A.K. Hilo, A.R. Abu Talib, A. Acosta Iborra, M.T. Hameed Sultan, M.F. Abdul Hamid, Effect of corrugated wall combined with backward-facing step channel on fluid flow and heat transfer, *Energy*. 190 (2020). <https://doi.org/10.1016/j.energy.2019.116294>.
- [9] Z. Yu Zhao, B. Han, X. Wang, Q. Cheng Zhang, T.J. Lu, Out-of-plane compression of Ti-6Al-4V sandwich panels with corrugated channel cores, *Mater Des*. 137 (2018) 463–472. <https://doi.org/10.1016/j.matdes.2017.10.055>.
- [10] H.H. Afrouzi, M. Ahmadian, A. Moshfegh, D. Toghraie, A. Javadzadegan, Statistical analysis of pulsating non-Newtonian flow in a corrugated channel using Lattice-Boltzmann method, *Physica A: Statistical Mechanics and Its Applications*. 535 (2019). <https://doi.org/10.1016/j.physa.2019.122486>.
- [11] X. Zhu, F. Haglind, Computational fluid dynamics modeling of liquid–gas flow patterns and hydraulics in the cross-corrugated channel of a plate heat exchanger, *International Journal of Multiphase Flow*. 122 (2020). <https://doi.org/10.1016/j.ijmultiphaseflow.2019.103163>.

- [12] D.E. ALNAK, Thermohydraulic performance study of different square baffle angles in cross-corrugated channel, *J Energy Storage*. 28 (2020). <https://doi.org/10.1016/j.est.2020.101295>.
- [13] E. Ünal, H. Ahn, E. Sorguven, Experimental investigation on flows in a corrugated channel, *Journal of Fluids Engineering, Transactions of the ASME*. 138 (2016). <https://doi.org/10.1115/1.4032754>.
- [14] P. Naphon, Effect of corrugated plates in an in-phase arrangement on the heat transfer and flow developments, *Int J Heat Mass Transf*. 51 (2008) 3963–3971. <https://doi.org/10.1016/j.ijheatmasstransfer.2007.11.050>.
- [15] P. Naphon, Heat transfer characteristics and pressure drop in channel with V corrugated upper and lower plates, *Energy Convers Manag*. 48 (2007) 1516–1524. <https://doi.org/10.1016/j.enconman.2006.11.020>.
- [16] P. Naphon, Effect of wavy plate geometry configurations on the temperature and flow distributions, *International Communications in Heat and Mass Transfer*. 36 (2009) 942–946. <https://doi.org/10.1016/j.icheatmasstransfer.2009.05.007>.
- [17] I. v. Miroshnichenko, M.A. Sheremet, I. Pop, A. Ishak, Convective heat transfer of micropolar fluid in a horizontal wavy channel under the local heating, *Int J Mech Sci*. 128–129 (2017) 541–549. <https://doi.org/10.1016/j.ijmecsci.2017.05.013>.
- [18] A.M. Hussein, Adaptive Neuro-Fuzzy Inference System of friction factor and heat transfer nanofluid turbulent flow in a heated tube, *Case Studies in Thermal Engineering*. 8 (2016) 94–104. <https://doi.org/10.1016/j.csite.2016.06.001>.
- [19] A.M. Hussein, H.K. Dawood, R.A. Bakara, K. Kadirgamaa, Numerical study on turbulent forced convective heat transfer using nanofluids TiO<sub>2</sub> in an automotive cooling system, *Case Studies in Thermal Engineering*. 9 (2017) 72–78. <https://doi.org/10.1016/j.csite.2016.11.005>.
- [20] V. Bianco, O. Manca, S. Nardini, Numerical investigation on nanofluids turbulent convection heat transfer inside a circular tube, *International Journal of Thermal Sciences*. 50 (2011) 341–349. <https://doi.org/10.1016/j.ijthermalsci.2010.03.008>.
- [21] H.A. Mohammed, A.N. Al-Shamani, J.M. Sheriff, Thermal and hydraulic characteristics of turbulent nanofluids flow in a rib-groove channel, *International Communications in Heat and Mass Transfer*. 39 (2012) 1584–1594. <https://doi.org/10.1016/j.icheatmasstransfer.2012.10.020>.
- [22] W. Yu, H. Xie, A review on nanofluids: Preparation, stability mechanisms, and applications, *J Nanomater*. 2012 (2012). <https://doi.org/10.1155/2012/435873>.
- [23] M. Rostamani, S.F. Hosseinizadeh, M. Gorji, J.M. Khodadadi, Numerical study of turbulent forced convection flow of nanofluids in a long horizontal duct considering variable properties, *International Communications in Heat and Mass Transfer*. 37 (2010) 1426–1431. <https://doi.org/10.1016/j.icheatmasstransfer.2010.08.007>.
- [24] S.A. Moshizi, A. Malvandi, D.D. Ganji, I. Pop, A two-phase theoretical study of Al<sub>2</sub>O<sub>3</sub>-water nanofluid flow inside a concentric pipe with heat generation/absorption, *International Journal of Thermal Sciences*. 84 (2014) 347–357. <https://doi.org/10.1016/j.ijthermalsci.2014.06.012>.

- [25] B. Takabi, H. Shokouhmand, Effects of Al<sub>2</sub>O<sub>3</sub>-Cu/water hybrid nanofluid on heat transfer and flow characteristics in turbulent regime, *International Journal of Modern Physics C*. 26 (2015). <https://doi.org/10.1142/S0129183115500473>.
- [26] M. Shahul Hameed, S. Suresh, R.K. Singh, Comparative study of heat transfer and friction characteristics of water-based Alumina-copper and Alumina-CNT hybrid nanofluids in laminar flow through pipes, *J Therm Anal Calorim*. 136 (2019) 243–253. <https://doi.org/10.1007/s10973-018-7898-z>.
- [27] S.K. Singh, J. Sarkar, Experimental hydrothermal characteristics of concentric tube heat exchanger with V-cut twisted tape turbulator using PCM dispersed mono/hybrid nanofluids, *Experimental Heat Transfer*. 34 (2021) 421–442. <https://doi.org/10.1080/08916152.2020.1772412>.
- [28] D. Madhesh, S. Kalaiselvam, Experimental analysis of hybrid nanofluid as a coolant, in: *Procedia Eng*, Elsevier Ltd, 2014; pp. 1667–1675. <https://doi.org/10.1016/j.proeng.2014.12.317>.
- [29] S. Suresh, K.P. Venkataraj, P. Selvakumar, M. Chandrasekar, Effect of Al<sub>2</sub>O<sub>3</sub>-Cu/water hybrid nanofluid in heat transfer, *Exp Therm Fluid Sci*. 38 (2012) 54–60. <https://doi.org/10.1016/j.expthermflusci.2011.11.007>.
- [30] J.A. Eastman, S.R. Phillpot, S.U.S. Choi, P. Keblinski, Thermal transport in nanofluids, *Annu Rev Mater Res*. 34 (2004) 219–246. <https://doi.org/10.1146/annurev.matsci.34.052803.090621>.
- [31] J. Sarkar, A critical review on convective heat transfer correlations of nanofluids, *Renewable and Sustainable Energy Reviews*. 15 (2011) 3271–3277. <https://doi.org/10.1016/j.rser.2011.04.025>.
- [32] M.M. Klazly, G. Bognár, Investigation of convective heat transfer enhancement for nanofluid flow over flat plate, in: *J Phys Conf Ser*, Institute of Physics Publishing, 2020. <https://doi.org/10.1088/1742-6596/1564/1/012007>.
- [33] A. Bibi, H. Xu, Q. Sun, I. Pop, Q. Zhao, Free convection of a hybrid nanofluid past a vertical plate embedded in a porous medium with anisotropic permeability, *Int J Numer Methods Heat Fluid Flow*. 22 (2020) 4083–4101. <https://doi.org/10.1108/HFF-10-2019-0799>.
- [34] B. Takabi, H. Shokouhmand, Effects of Al<sub>2</sub>O<sub>3</sub>-Cu/water hybrid nanofluid on heat transfer and flow characteristics in turbulent regime, *International Journal of Modern Physics C*. 26 (2015). <https://doi.org/10.1142/S0129183115500473>.
- [35] Y. Xuan, W. Roetzel, Conceptions for heat transfer correlation of nanofluids, n.d. [www.elsevier.com/locate/ijhmt](http://www.elsevier.com/locate/ijhmt).
- [36] H.C. Brinkman, The viscosity of concentrated suspensions and solutions, *J Chem Phys*. 20 (1952) 571. <https://doi.org/10.1063/1.1700493>.
- [37] T. Hayat, S. Nadeem, Heat transfer enhancement with Ag-CuO/water hybrid nanofluid, *Results Phys*. 7 (2017) 2317–2324. <https://doi.org/10.1016/j.rinp.2017.06.034>.
- [38] R.S. Vajjha, D.K. Das, D.P. Kulkarni, Development of new correlations for convective heat transfer and friction factor in turbulent regime for nanofluids, *Int J Heat Mass Transf*. 53 (2010) 4607–4618. <https://doi.org/10.1016/j.ijheatmasstransfer.2010.06.032>.
- [39] O.A. Akbari, D. Toghraie, A. Karimipour, M.R. Safaei, M. Goodarzi, H. Alipour, M. Dahari, Investigation of rib's height effect on heat transfer and flow parameters of laminar water-Al<sub>2</sub>O<sub>3</sub>



nanofluid in a rib-microchannel, *Appl Math Comput.* 290 (2016) 135–153.  
<https://doi.org/10.1016/j.amc.2016.05.053>.

- [40] S. Dinarvand, M.N. Rostami, I. Pop, A novel hybridity model for TiO<sub>2</sub>-CuO/water hybrid nanofluid flow over a static/moving wedge or corner, *Sci Rep.* 9 (2019).  
<https://doi.org/10.1038/s41598-019-52720-6>.